

FINAL REPORT

U.S. Department of Energy

Development of Advanced In-Situ Techniques for Chemistry Monitoring and Corrosion Mitigation in SCWO Environments

Principal Investigator:

D. D. Macdonald
Center for Electrochemical Science and Technology
201 Steidle Building
The Pennsylvania State University
University Park, PA 16802

Co-Principal Investigator:

S. N. Lvov
The Department of Energy and Geo-Environmental Engineering,
Pennsylvania State University
University Park, PA 16802

Collaborators:

X. Y. Zhou, X. Wei, S. M. Ulyanov
The Energy Institute, Pennsylvania State University
The Department of Energy and Geo-Environmental Engineering,
Pennsylvania State University
University Park, PA 16802

L. Kriksunov

Current address: Director, Worldwide Technology,
Buckbee-Mears Cortland Inc.,
30 Kellogg Road,
Cortland, NY 13075

Project Number: 55171

Grant No. DE-FG07-96ER62303

Grant Project Officer: Dr. Roland Hirsch

Project Duration: 9/1/1996 – 3/31/2000

TABLE OF CONTENTS

Executive Summary	3
1. Research Objectives	4
References	5
2. Background	6
Potentiometric Measurement of pH	6
Electrochemical Noise Analysis (ENA)	7
3. Methods and Results	9
Development of Flow-through Thermocell and Electrochemical Sensors	9
Flow-through external pressure balanced reference electrode (FTEPBRE)	9
Flow-through hydrogen electrode (FTHE)	10
Flow-through YSZ pH electrode	10
Experimental Procedure	10
Evaluation of the HCl Association Constant and pH	10
Results and Discussions	12
4. Quantitative Measurement of Corrosion Rate via ENA	13
Hydrothermal electrochemical cell	15
Data acquisition system	16
Experimental Procedure	16
EN Measurements	16
Mass Loss Tests	16
SEM and EDAX Studies	17
Results and Discussion	17
Noise levels of potential and coupling current	17
Corrosion of Type 304SS in subcritical and supercritical aqueous solutions	18
Corrosion Rate and electrochemical noise recession	19
Stern-Geary relationship	20
Electrochemical noise analysis and polarization measurement	23
References	24
5. Effect of Pressure on Corrosion Rate	25
Theoretical Principles	26
References	31
6. Standardization of pH	31
Measurements of pH	31
pH Standards	34
Contributions of the Activity of Water	34
References	34
7. Relevance, Impact, and Technology Transfer	37
In-Situ Potentiometric Measurement of pH	37
In-Situ Measurement of Corrosion Rate via ENA	38
Effect of Pressure on Corrosion Rate	38
Standardization of the pH Scale	38
8. Project Productivity	38
9. Personnel Supported	39
10. Degrees Granted	39
11. Publications and Presentations	39

Executive Summary

The principal objective of this work was to develop sensing technologies and corrosion monitoring techniques for use in Super Critical Water Oxidation (SCWO) systems. SCWO is currently being considered as a volume reduction technology for the pretreatment of Mixed Low Level Nuclear Waste (MLLNW), in which the organic component is oxidized in a closed cycle system to produce CO₂ and other gaseous oxides, while leaving the radioactive elements concentrated in the ash. The technique makes use of water at super critical temperatures ($T > 374.15$ °C, but typically at 600 °C to 650 °C in the reaction zone) under highly oxidizing conditions that are achieved by maintaining a high fugacity of molecular oxygen in the system. The principal hurdle in the development of this important technology is the corrosion of the reactor materials. Very high corrosion rates have been observed for even the most corrosion resistant alloys (e.g., Alloy C-276), such that the practical implementation of SCWO remains questionable. A significant part of the problem can be traced to the lack of effective tools (sensors and monitors) for ascertaining the chemical, electrochemical, and corrosion parameters in the reaction zone and in other areas of the system where severe corrosion occurs. The work accomplished in the present project has significantly addressed this shortcoming.

The accomplishments of this three and one half year program can be summarized as follows.

- Advanced electrodes and sensors for *in-situ* potentiometric monitoring of pH in high subcritical and supercritical aqueous solutions have been developed. An experimental flow-through thermocell was fabricated to test the flow-through reference electrode, the flow-through hydrogen electrode, and the flow-through YSZ pH sensor. Using these sensors, we have made quantitative, “research grade” pH measurements (with a precision of about ± 0.03) at temperatures as high as about 360 °C. We believe that these measurements are the first of their kind at temperatures just below the critical temperature of water.
- Additionally, semi-quantitative measurements of pH have been made in dilute HCl and NaOH solutions at temperatures as high as 528 °C, which we believe constitutes the highest temperature at which pH measurements have ever been made *in any system*. The measurements were made using a (Pt)Ag/O₂/YSZ sensor and an external pressure balanced reference electrode (EPBRE). The precision of these pH measurements (± 0.2) is such that they are suitable for plant monitoring purposes.
- An approach has been developed for the experimental evaluation of the association constants for 1-1 aqueous electrolytes using a flow-through electrochemical thermocell. The thermocell consists of a flow-through Pt(H₂) electrode and a flow-through external reference electrode. The viability of this method has been verified by using previously obtained emf data for aqueous HCl solutions at temperatures from 300 to 360°C and for pressures of 27.5 and 33.8 MPa. The derived values of the association constant of HCl(aq) are found to be in good agreement with literature data. pH values for 0.01 and 0.001 mol kg⁻¹ aqueous HCl solution are determined at temperatures and pressures of interest.
- An electrochemical noise sensor has been developed for the *in situ* measurement of corrosion rate in subcritical and supercritical aqueous systems, and the sensor has been evaluated in a contamination-free, flow-through hydrothermal electrochemical cell. The following conclusions were drawn from the present results:
 1. By measuring the coupling current for a pair of identical metal electrodes, and by simultaneously measuring the potential of one of the electrodes against a reference electrode, the corrosion rate can be evaluated quantitatively, as has been demonstrated in the past by many workers working at lower temperatures.
 2. The corrosion rate of Type 304 SS is a function of temperature and flow rate and the corrosion rate passes a maximum at 350°C, as determined by both ENA and mass loss experiments. The existence of the maximum is in agreement with earlier corrosion activity measurements (coupling current noise) on both carbon steel and stainless steel substrates in high subcritical and supercritical systems and with the predictions of a phenomenological model for the corrosion process.
 3. The inverse noise resistance is found to be proportional to corrosion rate evaluated from mass loss tests. This proportionality is found to exist over a wide range of conditions, i.e. for temperatures from 150 to 390°C and for flow rates from 0.375 to 1.00 ml/min.
 4. The Stern-Geary equation is a good approximation for the relationship between polarization resistance and corrosion current density for temperatures greater than 150°C.

5. Three electrode electrochemical noise techniques, as developed in this program, are effective in monitoring corrosion rate quantitatively in super critical aqueous systems. To our knowledge, this is the first instance that quantitative monitoring of corrosion rate at temperatures above the critical temperature has been demonstrated in *any* system.

A model has been developed for estimating the effect of pressure on reaction rates, including corrosion reactions, in high subcritical and supercritical aqueous systems. The model takes into account the effect of pressure on the activation process, on the volumetric concentrations of the reactants, and on the dissociation of HCl. The predictions of the model have been tested against experimental data for the corrosion of Type 1013 carbon steel in oxygenated (0.006 ppm O₂), supercritical water (T = 481 °C) over the pressure range from 2500 psi to 3500 psi. Satisfactory agreement is obtained between theory and experiment. The model is then used to explore the effects of pressure excursions on materials selection experiments, with the following findings:

1. Positive pressure excursions are predicted to increase the corrosion rate due to positive effects on activation, volumetric concentration, and HCl dissociation. A maximum increase in the corrosion rate of about 60 % is predicted for the highest temperature considered (T = 371.1 °C) upon increasing the pressure by 35.72 b (525 psi).
2. Negative pressure excursions are predicted to decrease the corrosion rate due to negative effects on activation, volumetric concentration, and HCl dissociation. A decrease in the corrosion rate of about 14 % is predicted for the lowest temperature considered (T = 343.3 °C) upon decreasing the pressure by 61.24 b (900 psi). However, very large reductions in corrosion rate are predicted for the two highest temperatures (365.5 °C and 371.1 °C) upon decreasing the pressure in the system by 900 psi. This large decrease, which may be orders in magnitude, is due to the sharp decrease in the dielectric constant of the medium and hence is due to strong decreases in the dissociation constants for water and hydrochloric acid as the temperature approaches the critical value.

These calculations further suggest that considerable relief from corrosion may be obtained by operating a SCWO reactor at reduced pressures. However, this would be at the expense of through put.

Following previous work, a pH standard for use at supercritical temperatures has been proposed, based upon the calculated values for the pH in a standard, 0.01 m HCl solution as a function of temperature. The contribution of the activity of water to the measured pH at high sub critical and at super critical temperatures has been explored and is shown to be of secondary importance.

The project has achieved all objectives, with the exception that we were unable to install some of the sensors into a fully operating SCWO system. This was because the current sensors were judged to be too fragile to operate under plant conditions and because of difficulties in scheduling the insertion of the sensors in the reactor at INEEL. However, a follow-on proposal has been submitted to EMSP emphasizing the development of rugged sensors that will be suitable for SCWO plant monitoring.

Finally, some of the techniques developed in this program have been used by the PI, acting as an advisor to Stone & Webster Engineering Corp. and the US Army, in the destruction of VX hydrolysate. This high visibility program, which entails the construction of a SCWO reactor at Newport, Indiana, results from an agreement between the US and Russia for the destruction of chemical agents. The contribution from the present program to the US Army effort was the development of the theory and model for assessing the impact of pressure on the rate of corrosion of metals and alloys in super critical aqueous systems. The model was used to correct corrosion rates measured in the laboratory to the process conditions that are envisioned to exist in the Newport reactor.

1. Research Objectives

Super Critical Water Oxidation (SCWO) is a promising technology for destroying highly toxic organic waste (including physiological agents) and for reducing the volume of low-level nuclear waste. For example, SCWO has been chosen by the US Army to destroy VX hydrolysate (product obtained by hydrolyzing the chemical agent VX with caustic) and a facility for meeting this goal is now being constructed in Newport, Indiana. The US Navy has also explored SCWO for destroying shipboard waste, including oils and greases, solvents, and paints. Various commercial pilot plant facilities have been built in the United States, Japan, and Europe, with the goal of demonstrating the efficacy of the method for destroying resilient organic waste. A variant of SCWO that operates under less severe conditions has been developed by SRI International in the form of Assisted Hydrothermal Oxidation (AHO). This technology is now offered on a

commercial basis by Mitsubishi Heavy Industries, who operate a commercial pilot plant in Nagasaki, Japan. Given the increasing sensitivity of regulatory agencies and the general public to toxic waste, there is little doubt that the commercial and governmental application of SCWO will expand rapidly in the foreseeable future.

SCWO offers a number of unique advantages over other waste destruction technologies, such as incineration and pyrolysis (e.g., in plasmas). These advantages include:

- Zero emissions to the environment.
- Very high destruction efficiencies (> 99.999 %), for even the most resilient waste.
- Relatively low cost.
- Remote siting through minimal need for services (electricity, etc.).

Nevertheless, the full and effective implementation of SCWO faces major challenges, depending upon the nature of the waste. Perhaps the greatest challenge is the selection of materials that can withstand the harsh oxidizing conditions that exist in the reactor and in downstream components. In light of the fact that no empirical materials selection databases exist for choosing materials of construction, a major problem inhibiting the wide implementation of SCWO is the lack of fundamental knowledge about various physico-chemical and corrosion processes in SCW environments.

As the result of research carried out in this program over the past three years, we have developed new chemical and corrosion sensors for use in high subcritical and supercritical aqueous environments. The precision and readability of the sensors have been significantly improved over previously available devices and the fundamental thermodynamic and corrosion properties of supercritical aqueous system can now be more accurately measured over a wide range of temperatures and pressures. In particular, flow-through yttria-stabilized zirconia (YSZ) pH and external reference electrodes have been developed. Potentiometric measurements were conducted to determine the pH of dilute hydrochloric acid (from 0.001 to 0.01 mol kg⁻¹) at temperatures up to 400°C. High precision potential data were obtained with a variation of ± 3 mV. The diffusion potentials were determined using available thermodynamic data and conductivity data found in literature. The diffusion potential values were then used to correct the potential measured using the YSZ pH electrode against the reference electrode. The association constant for hydrochloric acid was then evaluated from the corrected potential data. The results have been compared with available literature data and good agreement between experimentally measured and literature data have been observed.

Using a (Pt)Ag/O₂/YSZ pH sensor and an external pressure balanced reference electrode (EPBRE) of the type that we developed in previous programs, we have measured the pH of dilute HCl and NaOH solutions to 528 °C. These measurements, which set a record for the upper temperature, are of plant monitoring quality (± 0.2 pH units) and demonstrate the feasibility of monitoring pH in low-density super critical aqueous environments that are typical of those that exist in SCWO systems. We also demonstrated the feasibility of using pH measurements to monitor the destruction of a resilient organic waste (CCl₄) in SCW at temperature of 525 °C; a finding that could have important implications for future SCWO technology.

We have also continued the development of electrochemical noise analysis (ENA), which is more accurately termed electrochemical emission spectroscopy (EES), as a means of measuring *in situ* the rate of corrosion of metals and alloys in high subcritical and supercritical aqueous solutions. Our original work [1,2] focused on developing two-electrode, corrosion activity sensors, which were shown to permit accurate monitoring of the noise in the coupling current between two identical specimens in aqueous systems at supercritical temperatures. However, three electrode systems that monitor the noise in both the coupling current and the potential between one of the specimens and a suitable reference electrode have been in common use under ambient conditions for about two decades. The advantage of the three-electrode system is that it provides a measure of the “noise resistance”, which may be equated with the polarization resistance under specific conditions. The polarization resistance, in turn, may be used to calculate the corrosion current density and hence the instantaneous corrosion rate.

Following our previous work [3], we also addressed the issue of choosing the best pH scale for supercritical aqueous systems, because standardization of the scale will become essential if pH measurements from different groups are to be compared. Contrary to the situation that exists at temperatures below 300 °C, no strong acid/weak base or weak acid/strong base buffers are available for use in high subcritical and supercritical aqueous systems. Accordingly, the establishment of “standard” pH solutions is a matter of high priority.

Finally, while the theory for the effect of temperature on the corrosion rate of metals in high subcritical and supercritical aqueous solutions has been developed extensively [4], much less emphasis has been placed upon developing a comprehensive theory for the effect of pressure. Such a theory has been developed in the present program and has been used to assess the effect of pressure on the rates of corrosion of

candidate liner materials for the SCWO reactor being developed by the US Army in Newport, IN, for the destruction of VX hydrolysate.

References

1. C. Liu, D. D. Macdonald, E. Medina, J. Villa, and J. Bueno, "Probing Corrosion Activity in High Subcritical and Supercritical Water Through Electrochemical Noise Analysis", *Corrosion*, **50**, 687 (1994).
2. D. D. Macdonald, C. Liu, and M. P. Manahan, Sr., "Electrochemical Noise Measurements on Carbon Stainless Steels in High Subcritical and Supercritical Aqueous Environments", *ASTM STP-1277*, p. 247-265 (1996).
3. D. D. Macdonald, H. Arthur, R. Biswas, K. Eklund, N. Hara, G. Kelkar, L. Kriksunov, C. Liu, S. N. Lvov, and J. Mankowski, "Supercritical Oxidation Studies: Understanding the Chemistry and Electrochemistry of SCWO Systems", Final Progress Report to the US Army Research Office, Grant Nos. DAAL 03-92-G-0397 and DAAH 04-93-G-0150, February 1997.
4. L. Kriksunov and D. D. Macdonald, *J. Electrochem. Soc.*, "Corrosion in Supercritical Water Oxidation Systems: A Phenomenological Analysis", *J. Electrochem. Soc.*, **142**, 4069 (1995).

2. Background

Due to their unusual properties, high subcritical and supercritical aqueous solutions have many important industrial applications. One of the important applications of SCW is as a reaction medium in supercritical water oxidation (SCWO) technology, especially for eliminating various military organic wastes. However, the currently poor knowledge of the fundamental properties of supercritical aqueous solutions hinders the efficient application of this process. Furthermore, high subcritical and supercritical aqueous solutions are extremely corrosive toward metallic components. In many practical cases, the use of high subcritical and supercritical aqueous solutions is limited by corrosion problems. Development of *in-situ* techniques for measuring electrochemical parameters and monitoring corrosion processes in high subcritical and supercritical environments will not only benefit power generating, chemical, geothermal, oil refining, and supercritical water oxidation industries in terms of corrosion control, but will also offer unique and powerful tools for elucidating mechanisms of metallic corrosion under extreme environmental conditions.

The present work was aimed at developing:

- Techniques for the accurate potentiometric measurement of pH under prototypical SCWO reactor conditions;
- ENA technologies for quantitatively measuring corrosion rate in high subcritical and supercritical systems;
- A theory for the effect of pressure on the corrosion rates of materials in high subcritical and supercritical systems; and
- The establishment of a viable pH standard for high subcritical and especially supercritical systems.

Potentiometric Measurement of pH.

The measurement of pH in high temperature aqueous systems has been a major challenge in physical chemistry and in the power generation industry for over the five decades, and accurate pH measurements are still not routinely performed at temperatures above 100°C. However, over the past 30 years, several significant developments have been made to improve pH measurement techniques in high temperature subcritical and supercritical aqueous solutions.

Initial studies were focused on hydrogen concentration cells and on the Pd_xH|H⁺ system. These systems were extensively investigated by Dobson et al. [1], Macdonald et al. [2], Sweeton et al. [3], Mesmer et al. [4], and Wesolowski et al. [5]. The hydrogen concentration cells were employed to measure thermodynamic properties of aqueous solutions at temperatures up to 300°C, including the ionic product of water, the acid/base dissociation constant, and ion transport numbers.

Another very important development was the invention of a pH sensing electrode by Niedrach et al. [6,7], based on an oxygen ion conducting ceramic, yttria stabilized zirconia (YSZ). Bourcier et al. [8] measured pH using this same type of YSZ electrode at temperatures up to 275°C. Macdonald et al. [9,10] explored the YSZ electrode for measuring pH in high temperature subcritical and supercritical aqueous

systems at temperatures up to 375°C, using the Hg|HgO|YSZ|H⁺, H₂O electrochemical system. Lvov et al. [11] measured the pH of dilute ammonia solutions at temperatures between 150 and 300°C. Ding and Seyfried [12] conducted electrochemical cell measurements using the YSZ electrodes at temperatures up to 400°C. It has been found that the YSZ electrode exhibits the same pH response as the H₂(Pt) electrode and can be employed as a primary pH sensor. However, the systems developed to date comprising a YSZ pH sensor and a reference electrode also exhibited irreversibility, drifts, and errors, in some cases up to ± 0.5 pH units. The authors concluded that such errors are related principally to the reference electrode.

In previous work, Lvov et al. [13, 14] developed a variety of flow-through electrochemical systems and probes for performing high temperature potentiometric and pH measurements at temperatures up to 400°C with an accuracy of ±10 mV or ± 0.1 pH units. Very recently, the flow-through reference electrode and flow-through Pt(H₂) pH sensor have been further improved [15]. As a result, high precision pH measurements with an uncertainty of ±3 mV or ±0.03 pH units (at 300 °C) can now be carried out. Moreover, pH reference systems that can be used for assessing the viability and accuracy of high-temperature pH sensors have been developed [16].

Electrochemical Noise Analysis (ENA)

Spontaneous fluctuations of electrode potential and current in an electrochemical system are known as “electrochemical noise” or “electrochemical emissions”. Electrochemical noise analysis (ENA), or electrochemical emission spectroscopy (EES) is unique among all electrochemical techniques used in corrosion research, because it can be conducted under open circuit corrosion conditions, in which no perturbation needs to be applied to the system. The application of a perturbation in potential or current by an external device inevitably leads to changes in system-specific properties. While electrochemical noise contains rich information on the processes occurring in an electrochemical system, and noting that the measurement of noise requires a comparatively simple experimental setup, the extraction of the required data (polarization resistance and corrosion rate) is neither easy nor straightforward.

Ever since electrochemical noise studies in corrosion science were first reported in the 1960s and 70s [17, 18], extensive work has been reported on the origins of the fluctuations in current and potential at a corroding interface. Earlier studies concentrated on exploring the correlation between potential, current, and other characteristics of EN and corrosion rate [19-21]. These methods proved suitable for studying localized corrosion, such as pitting and stress corrosion cracking. However, potential or current monitoring can only provide a qualitative assessment of corrosion activity, as noted above. Later work was directed towards simultaneously monitoring the potential and the coupling current between two identical electrodes [22-29]. The results of these studies show that this method can be used to quantitatively evaluate corrosion rate. The most important step in the method is the determination of the noise resistance (R_n), which is defined as the ratio of the standard deviations of the potential and coupling current fluctuations:

$$R_n = \frac{\mathbf{s}_E}{\mathbf{s}_I} \quad (2-1)$$

where \mathbf{s}_E is the standard deviation of the potential fluctuation and \mathbf{s}_I is the standard deviation of the coupling current fluctuation.

Eden et al [22] and Chen and Skerry [23] suggested that R_n was related to the polarization resistance, R_p , which is commonly determined by linear polarization measurements or by electrochemical impedance spectroscopy (EIS). Initially, R_n was thought to be analogous to R_p and hence that the corrosion current (I_{corr}) could be evaluated using the Stern-Geary relationship [22, 23]:

$$I_{corr} = B \left(\frac{1}{R_p} \right) \quad (2-2)$$

It was later found that, in reality, R_n was not always equal to R_p , but rather that R_n is related to R_p indirectly. Bertocci et al [30] derived the relation between R_n and the spectral resistance, R_{sn} , as

$$R_n = \left(\frac{\int_{f_{min}}^{f_{max}} \Psi_I(f) R_{sn}^2(f) df}{\int_{f_{min}}^{f_{max}} \Psi_I(f) df} \right)^{1/2} \quad (2-3)$$

where $\Psi_I(f)$ is the power spectrum density (PSD) of the coupling current, f is the frequency in Hz, f_{min} is the lower limit frequency equal to the inverse measurement time, f_{max} is the higher limit frequency equal to one-half of the sampling frequency. The spectral resistance itself is defined by:

$$R_{sn} = \left(\frac{\Psi_V(f)}{\Psi_I(f)} \right)^{1/2} \quad (2-4)$$

where $\Psi_V(f)$ is the PSD of potential. If f_{max} is sufficiently low, R_n can be expressed by:

$$R_n = R_{sn}(f \rightarrow 0) \quad (2-5)$$

Through theoretical analysis involving minimal assumptions, Bertocci et al. [30,31] found that for the situation where: 1) The electrochemical noise sensor consisted of two identical coupled electrodes and a noiseless reference electrode; 2) instrumentation noise is negligible compared to the “true” electrochemical noise; and 3) the solution resistance is negligible compared to the electrode impedance, the following equalities existed:

$$R_n = R_{sn}(f \rightarrow 0) = Z(f=0) = R_p \quad (2-6)$$

where $Z(f=0)$ is the electrochemical impedance at zero frequency. This relationship was verified experimentally [27, 28] for the cases of bare electrodes and coated electrodes with defects. Note that there were other cases in which the above relationship did not exist [24-29], because the underlying conditions were not completely satisfied.

Previously, very limited attempts have made to explore the possibility of using ENA to monitor corrosion at high temperatures. Thus, Liu et al. [32] measured the coupling current between two identical steel electrodes with the goal of developing a “corrosion activity” sensor. Macdonald et al. [33] measured the coupling current between a coated steel specimen with a stress corrosion crack and an external cathode. They found that the coupling current was a function of temperature, flow rate, and dissolved oxygen concentration. The amplitude of the coupling current, as measured with the corrosion activity sensor, passed through a maximum at a near-critical temperature. However, no exploratory effort has been made to quantitatively measure corrosion rate via ENA at high subcritical and at supercritical temperatures ($T > 374^\circ\text{C}$).

Our principal objective in the present task was to concentrate on fundamental studies of supercritical aqueous fluids, as well as on developing new corrosion monitoring concepts for use in SCWO systems. The precision and reliability of sensing techniques have been improved, and advanced electrochemical noise monitoring techniques for use in SCWO system have been developed. Several specific tasks were fulfilled in this aspect of the project: (i) Design and construction of a high temperature/high pressure test loop, test reactor, data acquisition system, electrochemical noise monitoring system, (ii) measurement and analysis of electrochemical noise in high subcritical and in supercritical aqueous solutions; (iii) calculation of the instantaneous corrosion rate.

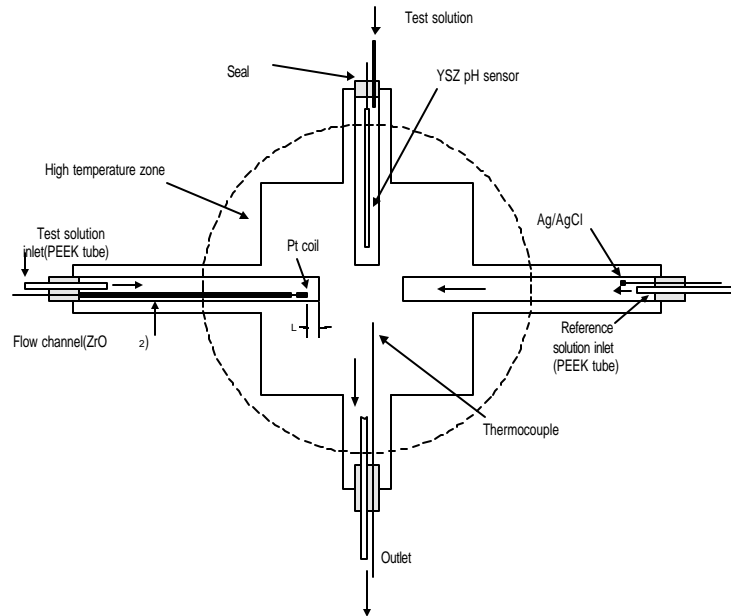


Figure 3-1. Schematic of the electrochemical thermocell module.

3. Methods and Results

Development of Flow-Through Thermocell and Electrochemical Sensors

The experimental system used for electrode testing is shown in Figure 3-1, and is much evolved from an earlier version described in Lvov, et al. [15]. The body is of a corrosion-resistant alloy, Titanium Gr5[®], and has four ports into which different components can be sealed for use at high pressures and temperatures. The components include a flow-through reference electrode, a flow-through hydrogen (Pt) electrode, an yttria-stabilized zirconia electrode, and a thermocouple. The design has a four-way, once-through pumped fluid circulation system that permits the solution to be pumped through the electrodes at rates that are sufficiently fast to counter thermal diffusion, so that no concentration gradients result from the Soret effect, but at a slow enough rate that the temperature gradient is maintained. Only the sensing portion of the system needs to be, and is, maintained at controlled temperatures and pressures. The purity and concentration of the solutions are maintained by both rapid renewal, due to the flow rate being sufficiently high that contamination by dissolution (corrosion) of the system is negligible, and also by contact of the low temperature input flow with only glass and Teflon[®]. Furthermore, the high temperature inflow and outflow contact only zirconia, platinum, and the alloy, Titanium Gr5[®]. This system is suitable for conditions up to at least 450°C and 40 MPa.

Flow-through external pressure balanced reference electrode (FTEPBRE)

The design of the FTEPBRE (Figure 3-2a) was similar to one described in Refs. 13 and 14. The stainless steel tube contained an inner tube, which comprises a shrinkable PTFE tube in the low temperature section and a ZrO₂ tube in the high temperature section. A Ag|AgCl electroactive element and a PEEK plastic inlet tube were placed into the heat-shrinkable PTFE tube. The reference solution (0.1 m NaCl) from the PEEK tube first flows through the PTFE tube and then through the ZrO₂ ceramic tube.

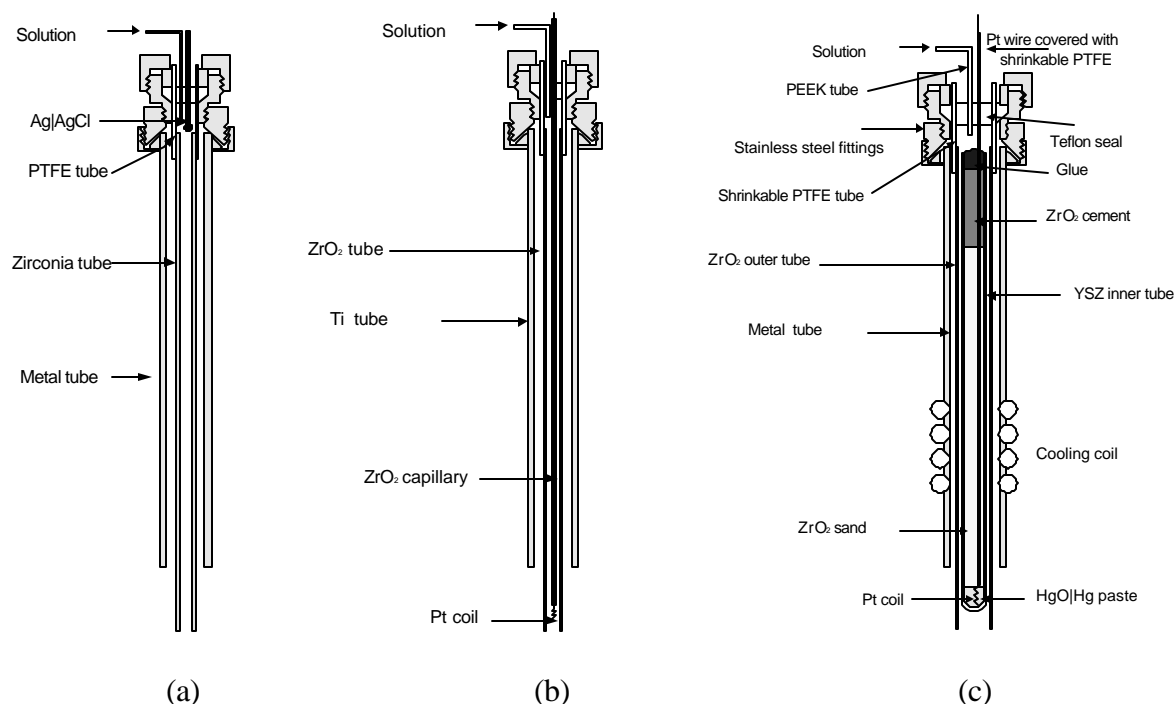


Figure 3-2. Design for flow-through external pressure balanced reference electrode (a), the flow-through external pressure balanced reference electrode, (b) flow through hydrogen electrode, and (c) the flow-through YSZ pH sensor.

Flow-through hydrogen electrode (FTHE)

A similar design was used for the flow-through hydrogen electrode (FTPHE) (Figure 3-2b). There exist three distinct features of the FTHE: (1) The high temperature tip of the electrode was coiled and platinized, with about half of the total length of the Pt wire (50 cm) being used to make this tightly coiled component, whose dimensions were 1.5 cm in length and 1.5 mm in diameter; (2) the remaining Pt wire was

first covered with a ZrO₂ film, which was electrophoretically deposited from a ZrO₂ sol (1.3% Yttrium, 18% ZrO₂, ALFA AESAR), and then was covered with a shrinkable PTFE in the low temperature section and with a thin Al₂O₃ ceramic tube (0.2 m length) in the high temperature section. The space inside the tube was filled with ZrO₂ cement, which was fired at 600°C. By this means, the contribution of the low temperature section of the Pt wire to the measured potential was eliminated; (3) the distance from the tip of the Pt coil to the hot end of the ZrO₂ tube was about 10 mm; this distance was estimated from hydrodynamic calculations as described below. The inner diameter of the ZrO₂ tube was 2.0 mm.

Flow-through YSZ pH electrode

The configuration of the YSZ electrode is illustrated in Figure 3-2c [34]. Crucial to this design is the dual sealing system. The YSZ tube at the top of the zirconia sand column is sealed with ceramic cement, which was baked at 600°C. Previously, particularly in research systems, YSZ pH electrodes have been installed in high-pressure systems with part of the ceramic tube that separates the high pressure/high temperature fluid from the external environment [35, 36] forming the pressure boundary. In the current design, the entire ceramic tube is within the metal-gland-sealed, high-pressure volume, with no ceramic wall serving as the pressure boundary. This design significantly increases the reliability and safety of high temperature pH measurements. We note, however, that the Pressure Vessel Code requires pressure boundaries to have properties that, invariably, can only be met by metal enclosures. Thus, ceramic sensors, which are installed in industrial systems (including some by this laboratory), are required to have (tough) metal pressure boundaries.

Experimental Procedure

Two Acuflo[®] HPLC pumps (Fisher Scientific), which provide flow rates from 0.1 to 10 ml min⁻¹ with an accuracy of 2% and that can sustain pressures up to 5000 psi (345 bar), were employed to pump the reference solutions through the FTEPBRE and the FTPHE. A constant system pressure was maintained via a backpressure regulator. The pressure was monitored visually using a standard pressure gauge and was also monitored electronically via a pressure transducer connected to a data acquisition system. The flow rates were measured using rotameters (Omega, accuracy 2%). Note that the tubing and cylinders of the pumps are made from plastics, while the pump pistons are made from glass. All of the tubes in the low temperature regions in our system were fabricated from PEEK. Therefore, in our modified experimental system, contamination of the solution from the reservoir to the hot ends of the ZrO₂ tubes was minimized and the solution composition was maintained at a known value.

An electrometer with an input impedance of 10¹⁴ Ω was used to measure the potential between the FTPHE and the FTEPBRE. An A/D converter monitored the potential output from the electrometer in a data acquisition system.

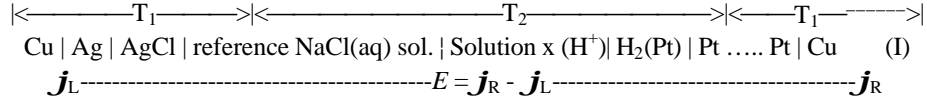
Copper tubes and shims were tightly fit into the gaps between the stainless steel cross and the four 450 W and 250 W band heaters. The high temperature part of the electrochemical cell was insulated with a ceramic fiber blanket. The cell temperature was measured using a K type thermocouple installed at the center of the cross and controlled using a CN9000 temperature controller (Omega). The variation in cell temperature was less than 1 K at the highest temperature of 400°C.

The test solutions directed into the electrochemical cell from the FTPHE side were either hydrochloric acid or HCl +NaCl solutions. The solutions were prepared by diluting a 0.1 m HCl standard solution with Millipore purified water (18.2 MΩ resistance) and then adding a precise amount of crystalline sodium chloride. The solutions were prepared using volumetric pipettes (50 and 25 ml, ±0.05 ml) and volumetric flasks (2 liter, ± 0.5 ml). The NaCl(s) was weighed using a Tare Model 300 electrical balance (Denver Instrument Co.). The accuracy of the solute concentration was ± 0.01% for NaCl and ± 0.1% for HCl. The reservoirs for the working solutions were purged with pure hydrogen (99.0%) and the reservoir containing the reference solution was purged with pure helium (99.0%).

At the beginning of each test, Solution 1 was pumped into the cell for about 3 hours, and then Solution 2 went through the same process. Another 3 hours after Solution 2 was pumped into the autoclave, Solution 1 was used again. The potential between the FTPHE and the FTEPBRE was recorded continuously using a data acquisition system. All of these measurements were carried out at a constant temperature.

Evaluation of the HCl Association Constant and pH

The following thermocell was previously developed in our laboratory for high temperature potentiometric measurement [13-15]:



where E is the cell emf, \mathbf{j}_R and \mathbf{j}_L are, respectively, the potentials at the right and left sides of the electrochemical system (I). As has been shown in Refs. [13-15], by using two similar (with respect to the solute) aqueous solutions (Solution 1 and Solution 2) having different analytical concentrations, and by measuring two corresponding emf values (E_1 and E_2), we can estimate the pH difference between the two solutions. The difference between E_1 and E_2 can also be expressed as [16]:

$$\Delta E_{1,2} = E_1 - E_2 = \frac{RT}{F} \ln \left\{ \frac{[\text{H}^+]_1 \mathbf{g}_1}{[\text{H}^+]_2 \mathbf{g}_2} \right\} + (E_{d,1} - E_{d,2}) \quad (3-1)$$

where $[\text{H}^+]_1$ and $[\text{H}^+]_2$ are the concentrations of H^+ in Solutions 1 and 2, respectively, \mathbf{g}_1 and \mathbf{g}_2 are the activity coefficients of H^+ in Solutions 1 and 2, and $E_{d,1}$ and $E_{d,2}$ are the diffusion potentials between the reference solution and Solution 1 and 2. Because the activity of H^+ is a function of the association constant of the dissolved electrolyte, we used this relationship to experimentally estimate the association constant for HCl and the pH for the aqueous electrolyte. As an example, we chose HCl(aq) solutions, which had already been experimentally investigated using Thermocell (I) [13]. Our approach is presented below.

In an HCl(aq) solution, the concentrations of H^+ , OH^- , Cl^- , and HCl^0 species are related by the following equations:

(a) Mass balance

$$[\text{H}^+] + [\text{HCl}^0] = m_{\text{HCl}} \quad (3-2)$$

(b) Electroneutrality

$$[\text{H}^+] = [\text{Cl}^-] + [\text{OH}^-] \quad (3-3)$$

(c) Association equilibrium of HCl

$$\frac{[\text{HCl}^0]}{[\text{H}^+][\text{Cl}^-] \mathbf{g}_{\pm}^2} = K_{\text{HCl}} \quad (3-4)$$

(d) Dissociation equilibrium of water

$$[\text{H}^+][\text{OH}^-] \mathbf{g}_{\pm}^2 = K_w a_w \quad (3-5)$$

where $[\text{H}^+]$, $[\text{OH}^-]$, $[\text{Cl}^-]$, and $[\text{HCl}^0]$ are concentrations of the corresponding species, m_{HCl} is the analytic concentration of HCl, \mathbf{g}_{\pm} is the activity coefficient, a_w is the activity of water, K_{HCl} is the association constant of HCl, and K_w is the dissociation constant of water. For dilute aqueous solutions, values for \mathbf{g}_{\pm} and a_w can be estimated, as described in Ref. [13, 14], using the second approximation of the Debye-Hückel theory [37]. Note that the activity coefficient of HCl^0 is assumed to be 1 and that this approximation does not give rise to any significant error in our calculations. Obviously, if the values of m_{HCl} , K_{HCl} , and K_w are given, the concentrations of the four species can be obtained by solving a set of four nonlinear Eqs. (3-2) to (3-5). By solving this problem for two HCl(aq) solutions with two analytical concentrations, $(m_{\text{HCl}})_1$ and $(m_{\text{HCl}})_2$, the $\Delta E_{1,2}$ value can be easily calculated from Eq. (3-1). However, if $(m_{\text{HCl}})_1$, $(m_{\text{HCl}})_2$, and K_w are given and $\Delta E_{1,2}$ is measured for two HCl(aq) solutions, K_{HCl} can be considered as a variable and hence can be determined from Eqs. (3-1) to (3-5). It should be noted that, in practice, knowledge of K_w is not important in the problem described above, and only $(m_{\text{HCl}})_1$, $(m_{\text{HCl}})_2$, and $\Delta E_{1,2}$ are the important input parameters that are required for estimating K_{HCl} . By combining Eqs. (3-2) to (3-5), we can derive an expression within which $[\text{H}^+]$ is considered to be a variable:

$$[\text{H}^+] = \frac{m_{\text{HCl}}}{K_{\text{HCl}} \mathbf{g}_{\pm}^2 [\text{H}^+] + 1} + \frac{K_w a_w}{[\text{H}^+]} \quad (3-6)$$

For a wide range of parameters (including ambient conditions and low-density supercritical fluid), $K_w \ll [\text{H}^+]$, so that Eq. (3-6) can be simplified to read

$$[\text{H}^+] = \frac{m_{\text{HCl}}}{K_{\text{HCl}} \mathbf{g}_{\pm}^2 [\text{H}^+] + 1} \quad (3-7)$$

We have found that Eq. (3-7) is very accurate at the temperatures and pressures of interest and can be used without any limitations. As can be seen from Eq.(3-7), if K_{HCl} is found, the pH can be calculated from the definition [38]:

$$pH = -\lg([\text{H}^+ \mathbf{g}_{\text{H}^+}]) \quad (3-8)$$

Because HCl(aq) solutions are completely dissociated under ambient conditions but are extensively associated in low-density, supercritical fluids, depending upon the prevailing conditions, we can estimate the sensitivity of our method for deriving the K_{HCl} values by measuring $\Delta E_{1,2}$. This analysis was performed by using Eqs. (3-1) and (3-7). Substituting Eq. (3-7) into Eq. (3-1), and assuming zero diffusion potentials (for simplicity's sake), $\Delta E_{1,2}$, as a function of K_{HCl} , can be calculated. In Figure 3-5, $\Delta E_{1,2} F / RT$ vs. K_{HCl} is plotted for a case of $(m_{\text{HCl}})_1 = 0.01 \text{ mol kg}^{-1}$ and $(m_{\text{HCl}})_2 = 0.001 \text{ mol kg}^{-1}$. As can be seen from Figure 3-4, if K_{HCl} is less than 10 or greater than 10^5 we are not able to precisely solve the speciation problem. However, this is not a problem for our technique. It is simply not possible to estimate the association constant, if the dissolved electrolyte is either completely dissociated (the association constant is very small) or completely associated (the association constant is very large).

In the above treatment of the speciation problem, we have ignored the diffusion potential, E_d . The diffusion potential is a significant issue in high temperature potentiometric and pH measurements, as has been discussed elsewhere [14, 39]. Briefly, we calculate the diffusion potentials using the available thermodynamic and transport property data. Details of our approach have been explained in a recent paper [39]. Because the diffusion potential is a function of speciation, E_d and K_{HCl} should be calculated in an iterative manner. First, we use Eq. (3-1), assuming that $E_d = 0$. Once the first approximation for K_{HCl} is found, we use the K_{HCl} value to estimate the speciation employing Eqs. (3-2) to (3-6). The calculated concentrations of the species are then used to estimate E_d , which is used in Eq.(3-1). This cycle is repeated until further iteration does not change the K_{HCl} and E_d values.

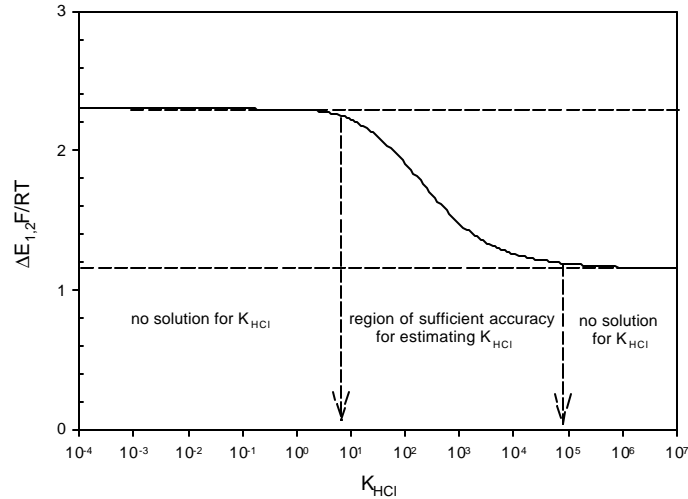


Figure 3-3. $\Delta E_{1,2} F / RT$ as a function of K_{HCl} : $(m_{\text{HCl}})_1 = 0.01 \text{ mol kg}^{-1}$ and $(m_{\text{HCl}})_2 = 0.001 \text{ mol kg}^{-1}$.

Results and discussions

We have developed a computer code based on the algorithm described above for determining the association constant, K_{HCl} , and the pH using Eqs. (3-1) to (3-5). The input data include the analytical concentrations of the two aqueous HCl solutions (0.01 mol kg^{-1} and $0.001 \text{ mol kg}^{-1}$) and the potential difference, $\Delta E_{1,2}$, which was taken from Ref.[13]. The precision of the $\Delta E_{1,2}$ measurements was estimated in

Ref. [13] to be within $\pm 3\text{-}10$ mV (± 6.5 mV average). The input data and results of our calculations are given in Table 3.1. The diffusion potentials are calculated using a recently developed computer code [39]. pH values are calculated using Eqs. (3-7) and (3-8).

As we note above, while making the sensitivity analyses, it was found that there are no mathematical solutions for K_{HCl} at temperatures below 300°C . That is because, when the temperature is low, almost all of the HCl molecules are dissociated. Note that at temperatures below 300°C , the pH values were calculated by multiplying the analytical HCl concentration by the corresponding activity coefficient. The precision of the calculated K_{HCl} values is a function of temperature and pressure, and has been estimated in the sensitivity analysis (see Figure 3-4) and taking into account the average experimental error of $\Delta E_{1,2}$ being equal to ± 6.5 mV.

Table 3-1. Experimentally measured potential differences, $\Delta E_{1,2}$ [13], and the calculated diffusion potentials, association constants, and pH of aqueous HCl solutions at temperatures between 25 to 360°C and pressure of 27.5 and 33.8 MPa.

T, $^\circ\text{C}$	P, MPa	$E_{d,1} - E_{d,2}$, mV	$\Delta E_{1,2}$, mV	$\lg(K_{\text{HCl}})$	pH	
					0.01 mol kg^{-1} HCl	0.001 mol kg^{-1} HCl
25	27.5	-2.9	64.5*	-	2.04	3.02
25	33.8	-3.9	61.4	-	2.04	3.02
100	27.5	2.8	81.0	-	2.05	3.02
200	27.5	4.5	97.8	-	2.07	3.02
300	27.5	4.4	100.3	1.84 ± 0.4	2.21 ± 0.10	3.06 ± 0.03
350	27.5	3.8	93.4	2.51 ± 0.3	2.40 ± 0.09	3.13 ± 0.03
350	33.8	3.6	97.4	1.99 ± 0.3	2.26 ± 0.06	3.07 ± 0.02
360	33.8	3.6	91.7	2.48 ± 0.3	2.39 ± 0.09	3.13 ± 0.04

(*) The experimental precision of measurements was estimated in Ref. [13] to within $\pm 3\text{-}10$ mV (± 6.5 mV average).

Another way to verify the accuracy of the estimated K_{HCl} values is to compare them with the data obtained by other methods, including conductivity, solubility, and calorimetric techniques. In Figures 3-5 and 3-6, we compare the $\lg(K_{\text{HCl}})$ values obtained in this work (Table 3-1) and the results from Ref.[16], which are presented as the empirical analytical equation:

$$\lg K_{\text{HCl}} = \mathbf{r}(255.63 - 192.62 \times \tilde{T}) + \mathbf{r}^2(-385.80 + 295.00 \times \tilde{T}) + \mathbf{r}^3(162.46 - 135.20 \times \tilde{T}) + 42.16 \times [\exp(-31.202 \times \mathbf{r} \times \tilde{T}) - 1] + 1.652 + 35.6 \times \tilde{T} - 0.221 \times \lg \tilde{T} - 1.744 \quad (3-9)$$

where \mathbf{r} is the density of water (in g/cm^3), $\tilde{T} = 10^3/T$, and T is the temperature in K. The empirical parameters of Eq. (3-9) were adjusted using available experimental data for the association constants of HCl(aq) (34 experimental points). The standard deviation of the fitting was found to be equal to 0.36 logarithmic units. Note that Eq. (3-9) was constructed in such a way that it has the correct zero-density limit. Therefore, the low-density extrapolation should be reliable.

The K_{HCl} values are calculated using Eq. (3-9) under isobaric conditions for pressures of 27.5 MPa (Figure 3-5) and 33.8 MPa (Figure 3-6). The lower and upper confidence regions of Eq. (3-9) are presented in Figure 3-5 and 3-6. Obviously, the confidence regions of our experimental results (error bars) overlap with the confidence regions of Eq. (3-9) and this fact confirms that our experimental data are reliable.

4. Quantitative Measurement of Corrosion Rate via ENA

There are two major difficulties in developing electrochemical sensors suitable for use in supercritical environments. The first is the sealing problem. The sensing electrodes should be exposed to the high temperature solution in which these electrodes are supposed to operate, but all other parts of the electrodes should not be exposed to the solutions. Furthermore, the sealing should be sufficiently effective, so as to not induce crevice corrosion. Secondly, with the exception of some precious metals, metals and alloys dissolve

readily under high temperature conditions and generate corrosion products that contaminate the tested solution. Accordingly, the composition of the solution in contact with the sensing electrodes might be substantially different from the composition of the initial (input) solution. In the worst case, the composition will change continuously during data acquisition and the electrochemical steady state may never be achieved. We employed a number of techniques in the present study to solve these problems .

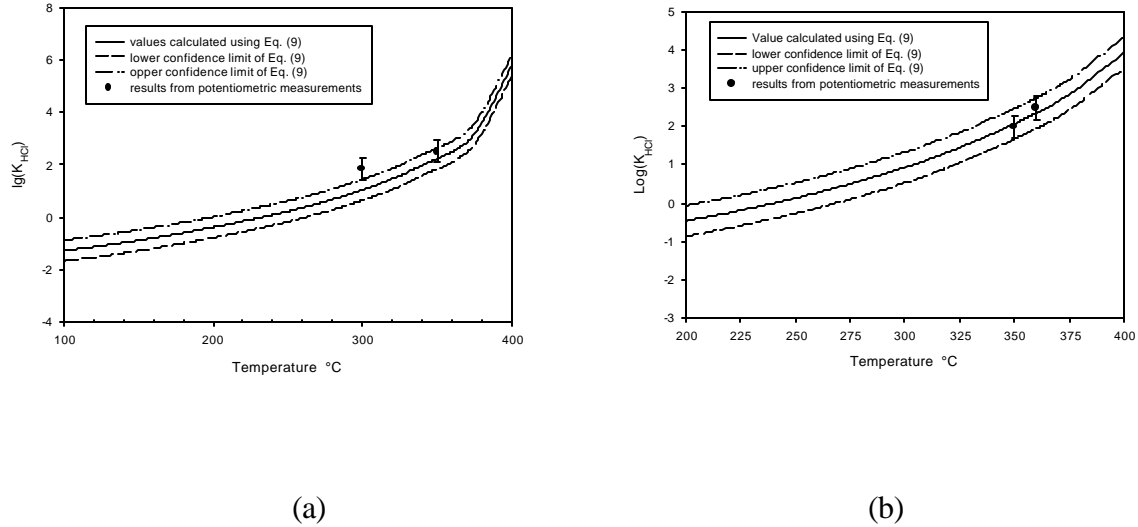


Figure 3-6. Comparison of $\lg(K_{HCl})$ obtained in this work and the values calculated by Eq. (3-9) at pressures of 27.5 MPa (a) and at 33.8 MPa (b).

The electrochemical noise sensor used here consisted of three electrodes. As shown in Figure 4-1, two of them were Type 304 stainless steel wires with a diameter of 0.50 mm taken from the same roll. The third electrode was a platinum wire, with a diameter of 0.50 mm. The wires were inserted into a three-hole ceramic tube and initially both ends of the wires were exposed. The distance between the holes was 1.5 mm. The extra space in the holes was filled with high temperature zirconia (ZrO_2) cement, which was also used as the sealant for ends of the tube. After the cement had dried under ambient conditions, the entire assembly was heat-treated in vacuum at 800°C for 24 hours.

After being heat-treated, at one end of the ceramic tube, each of the exposed wires was cut to assure that a length of 10 mm remained. These wires were then lightly polished, washed with acetone and de-ionized water, and subsequently dried. This part of the assembly was prepared for exposure to high temperature solutions. The other exposed parts of the wires were first covered with shrinkable PTFE tubing. The ends of the PTFE tubes were pre-etched using an oxidizing solution. A cement was used to fill the small gaps between the PTFE tube and the ceramic tube. These PTFE-shielded wires were then installed in standard CONAX glands. This part of the assembly was kept at ambient temperature in our experiment. In addition to the wires, a PEEK capillary, acting as the solution inlet, was also installed in the CONAX glands. Finally, the entire assembly was placed inside a flow channel made from a zirconia tube in the high temperature zone and from a shrinkable PTFE tube in the low temperature zone. Thus, the test solution from the PEEK capillary did not contact any metallic surface before reaching to the electrodes. The ends of the electrodes were located at a distance of 10 mm from the end of the outer zirconia tube, so that contamination from outside of the channel was impossible when there was solution flow in the channel.

Outside of the flow channel, a stainless steel tube was employed to maintain the sensor in the high pressure/temperature fluid. The stainless steel tube was connected to the CONAX glands at one end and to the hydrothermal cell at the other end. During the course of the present experiments, a test solution was fed from the PEEK inlet using a metal-free HPLC pump. Since the test solution only contacted plastic and ceramic surfaces, and because the solution was renewed constantly, solution contamination inside the flowing channel was minimized.

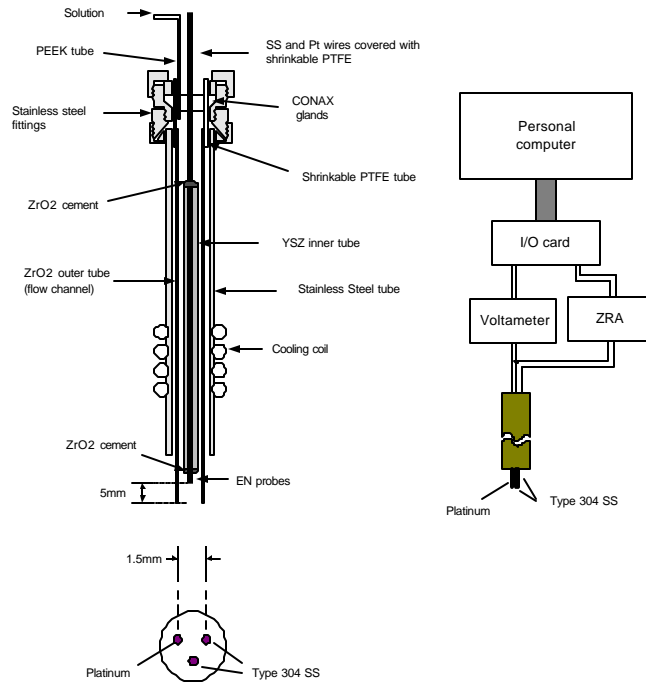


Figure 4-1. Schematic of the electrochemical noise sensor and data acquisition system.

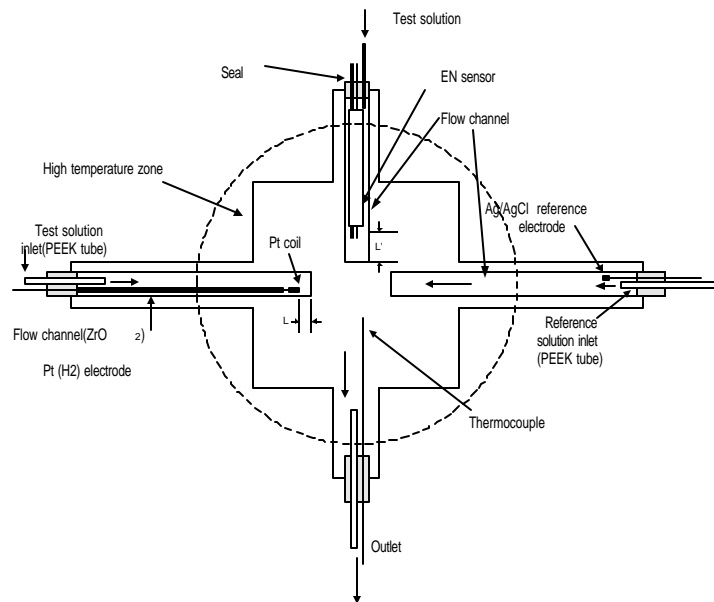


Figure 4-2. Schematic of hydrothermal electrochemical cell.

Hydrothermal electrochemical cell

A once-through, hydrothermal electrochemical cell (Figure 4-2), similar to the one described in Refs. [13-15], was used for the present experiments. The body of the cell was made from a stainless steel union cross with four ports: (1) A flow-through external reference electrode [15]; (2) the electrochemical noise sensor; (2) a flow-through hydrogen (Pt) electrode [15]; and (4) a solution outlet and a thermocouple. The

reference and Pt electrodes, located in zirconia channels, were employed for monitoring pH in the hydrogenated conditions.

Besides those features mentioned above, the hydrothermal electrochemical cell was heated with band heaters and was maintained at a pressure of 25 MPa with a pressure relief valve. The temperature and pressure were controlled to $\pm 0.2^\circ\text{C}$ and ± 0.1 MPa, respectively.

Data acquisition system

The coupling current between the two identical stainless steel wires of the EN sensor was measured with a zero resistance ammeter (ZRA) (Figure 4-1). The Pt wire of the EN sensor was employed as a low noise reference electrode. The potential of the coupled stainless steel electrodes, measured against the Pt electrode, was acquired using a programmable Keithley electrometer. The analog outputs of the electrometer and the ZRA were first transferred to an amplifier and were then converted into digital signals via a National Instrument A/D board operated by a LabView[®] program. For compromising the accuracy with the response speed of the data acquisition system, we chose a sampling frequency of 4 Hz and a sampling time of 512 seconds. In other words, each data set acquired consisted of 2048 readings.

To evaluate the noise level of the instrument, a dummy cell (electronic circuit) consisting of a resistor of 100 Ω or 10 K Ω , was measured with the data acquisition system. It was found that the noise level of the potential was less than 0.1 mV, and the noise level of the current was less than 2 nA.

Experimental Procedure

EN measurements

The first task of the experiments was to verify the reliability and accuracy of the pH monitoring system consisting of the flow-through reference and Pt electrodes. The method has been fully described in Ref. [15]. Basically, two hydrogen-saturated solutions, 0.1 mol kg⁻¹ NaCl + 0.01 mol kg⁻¹ HCl (sol.1) and 0.1 mol kg⁻¹ NaCl + 0.001 mol kg⁻¹ HCl (sol.2), were pumped into the flow channel of the Pt electrode consecutively. The solution that was pumped through the external reference electrode was always 0.1 mol kg⁻¹ NaCl from a reservoir purged with helium gas. The potentials of the Pt electrode against the reference electrode for both solutions were measured. The difference of the potentials for the two solutions were compared to the value calculated by [16]:

$$\frac{\Delta E - \Delta E_d}{\frac{RT}{F} \ln 10} = \lg\left(\frac{m_{\text{HCl}}(S1)}{m_{\text{HCl}}(S2)}\right) = -\Delta\text{pH} \quad (4-1)$$

where ΔE is the calculated potential difference, ΔE_d is the residual diffusion potential, $m_{\text{HCl}}(S1)$ and $m_{\text{HCl}}(S2)$ are the analytical concentration of HCl in solutions 1 and 2, respectively, and ΔpH is the pH difference of the two solutions at the temperature of interest. As an example, we found that the potential difference measured at 150°C was 75 mV \pm 2 mV, while the calculated value was 78 mV. Thus, the pH monitoring system was accurate and is capable of monitoring a pH difference of 0.05 units.

The second step was to acquire EN signals in 0.1 mol kg⁻¹ NaCl + 0.01 mol kg⁻¹ HCl while the pH monitoring system was in operation. The test solution was directed to the EN sensor and to the Pt electrode from a reservoir that was purged with high purity hydrogen gas. Note that all solutions were made from Millipore de-ionized water and reagent grade chemicals using Pyrex glassware and high precision balance ($\pm 0.0001\text{g}$). We tested the EN sensors at temperatures from 150 to 390°C and at flow rate from 0.375 to 1.0 ml/min. Note that one EN sensor was used for just one test at a specific temperature.

Mass loss tests

Mass loss tests were conducted in the same hydrothermal cell. Instead of an EN sensor, a stainless steel coil from the same roll of stainless steel wire as that used for the sensors was placed inside the ceramic channels. The coil was weighed prior to each test. After the test, the wire was cleaned with acetone in an ultrasonic cleaner, washed with acetone and de-ionized water, dried, and was then weighed again. The corrosion rate (I_{corr} in A/cm²) was evaluated by the equation:

$$I_{\text{corr}} = \frac{\Delta M}{M_0 AT} zF \quad (4-2)$$

where T is the time of exposure (in second) to the high temperature solution, A is the average of the initial and final surface areas of the coil (in cm^2), \mathbf{DM} is the mass loss (in grams), M_0 is the atomic mass, z is the oxidation number, and F is Faraday's constant.

SEM and EDAX studies

Scanning Electron Microscopy (SEM) was used to determine the surface morphology and thickness of the wires prior to and following the corrosion experiments. The SEM energy dispersive spectrometer (EDS) was used to determine the ratios between chromium, iron, and nickel in the fresh (un-corroded) and the corroded samples. These ratios were quantified by setting an 8-10 channel window centered on the main peak for each element and subsequently by calculating the ratios between the integrated surfaces.

Results and Discussion

Noise levels of potential and coupling current

As shown in Figure 43, there were drifts for both potential and coupling current. Thus, linear regression functions were generated for potential and current. Then the drifts were eliminated by

$$dE(t) = E_0(t) - E_{reg}(t) \quad (4-3)$$

and

$$dI(t) = I_0(t) - I_{reg}(t) \quad (4-4)$$

where $E_0(t)$ and $I_0(t)$ are respectively the original potential and current values, and $E_{reg}(t)$ and $I_{reg}(t)$ are the regression functions generated from the original values. $dE(t)$ and $dI(t)$ without drift are also presented in Figure 43. The standard deviations for both potential and current, s_E and s_I were calculated from $dE(t)$ and $dI(t)$, respectively, and the noise resistance (R_n) was calculated using Eq.(2-1).

Because the potential and current noise levels from the instrument were less than 0.1 mV and 2 nA, respectively, and were much lower than 10 mV and 10 μA , instrumentation noise was neglected.

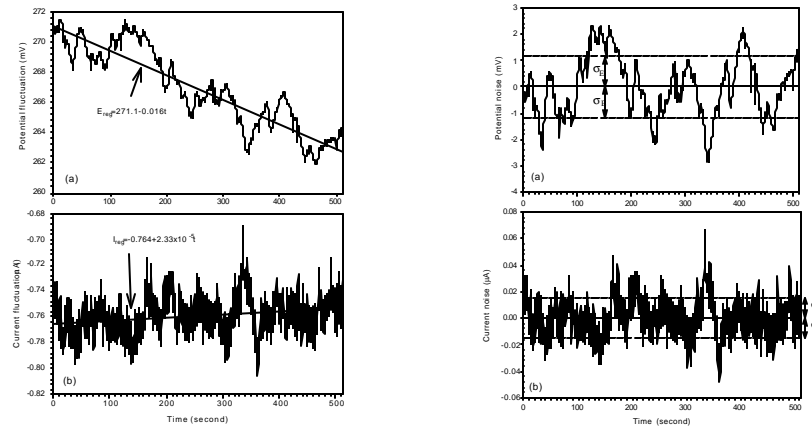


Figure 43. Original records of potential and coupling current acquired from an EN sensor at a temperature of 350°C, pressure of 25 MPa, and flow rate of 0.5 ml/min in hydrogenated 0.01 mol kg^{-1} HCl + 0.1 mol kg^{-1} NaCl (left frame) and after correction for drift (right frame).

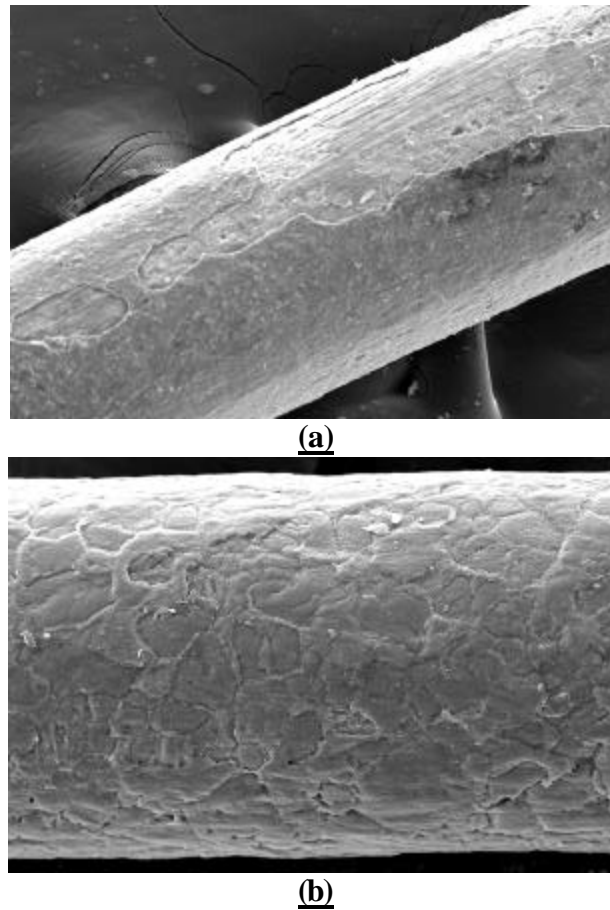


Figure 44. SEM micrographs: (a) sample tested at 150°C for 168 hours; (b) sample tested at 390°C for 1 hour.

Corrosion of Type 304 SS in subcritical and supercritical aqueous solutions

SEM examinations of the tested Type 304 wires (Figure 44a) revealed that at 150°C, localized corrosion occurred, but that this corrosion feature did not belong to a typical pitting corrosion. After a one week long test, no significant reduction in wire diameter was observed (Table 4-1). EDAX analyses (Table 4-1) indicate that Fe was depleted and Cr was enriched on the surface or sub-surface, possibly because of selective dissolution. At higher temperatures, Type 304 SS suffered from general corrosion (Figure 4-4b) that resulted in a considerable reduction in wire diameter (Table 4-1). The ratio of Cr to Fe was less than that for 150°C.

Table 4-1. Summary of the results of SEM and EDAX studies. The diameter was measured directly by SEM. The ratio of elements was obtained from EDAX analysis.

		Average wire diameter	Cr : Fe	Cr: Ni	Fe : Ni
(a)	uncorroded	490 ± 3 μm	0.46 : 1	4.7 : 1	10.0 : 1
(b)	150°C (1 week)	480 ± 5 μm	15.5 : 1	48.7 : 1	3.1 : 1
(c)	390°C (1 h)	350 ± 5 μm	8.6 : 1	19.9 : 1	2.3 : 1

By quantitatively analyzing Fe-Cr alloys using ESCA, Olefjord and Brox [40] found that the enrichment of Cr and the depletion of Fe on the surface and in the sub-surface area were functions of potential. The maximum enrichment of Cr in that study was found at a potential in the passive region close to the active-passive transition potential. There was some enrichment of Cr in the active region, but the enrichment was much less than that in the passive region.

Thus, for 150°C, the corrosion scenario seems to lie between active dissolution and complete passivity. The proposed scenario is that the system exhibits active dissolution and passivity simultaneously on the same surface, but within different regions, possibly reflecting the underlying grain structure. At higher temperatures, Type 304 SS is proposed to be in the active dissolution state. In this state, local anodic (metal oxidation) and cathodic (hydrogen evolution) partial reactions “flicker” across the surface under the constraint that the time averaged charge in both phases (metal and solution) must be zero.

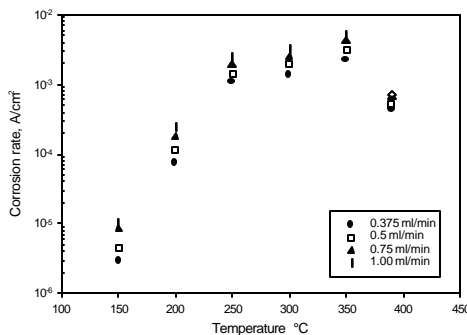


Figure 4.5. Corrosion rate (current) evaluated using mass loss tests as a function of temperature and flow rate.

If the anodic reaction has a greater probability of occurring at a particular point on the surface than does the cathodic reaction, then that area will become preferentially attacked. In this dynamic picture of the corroding interface, “general corrosion”, or “uniform attack”, corresponds to the extreme where there is equal probability of the partial anodic and cathodic reactions occurring at the same location. On the other hand, if the probability of anodic attack at any given point is unity, and hence the probability that the cathodic reaction occurs at the same location is zero, the pure “localized corrosion” is observed. Clearly, this scenario corresponds to the other extreme. In reality, a spectrum of corrosion states exists between these extremes.

The “flickering” of the local anodic and cathodic partial reactions, with the concomitant flickering of charge imbalance on both sides of the interface, is the source of the electrochemical noise. Because the instantaneous fluctuations in charge are likely controlled by the kinetics of the partial charge transfer reactions, it is reasonable to assume that the properties of the noise reflect the corrosion rate. Accordingly, we assume that the measured “noise resistance” (Eq. 2-1) is, in fact, a reasonable measure of the polarization resistance, provided that the lowest frequency component in the noise is at a sufficiently low frequency that the impedance is non-reactive.

The corrosion rate was found to be a function of temperature and, to a lesser extent, flow rate (Figure 4-5), in agreement with the earlier corrosion activity studies of Liu, et al. [32]. The corrosion rate is observed to pass through a maximum at 350°C. That the corrosion rate passes through a maximum at a near-critical temperature has been reported by other investigators [32, 33, 41]. The origin of the maximum has been well accounted for by the phenomenological model of Kriksunov and Macdonald [50], in terms of the competing effects of temperature on reaction rate constants and upon the density and dielectric constant of the medium. Thus, as the temperature is increased, the rate constants for the partial anodic and cathodic reactions increase exponentially, in accordance with Arrhenius’ law. However, the same increase in temperature, with the concomitant decrease in density and dielectric constant, results in a decrease in the volumetric concentrations of the reactants and in a decrease in the extent of dissociation of electrolytes (including HCl), particularly as the temperature transitions the critical temperature. Both of these phenomena result in a decrease in the reaction rate, with the result that the observed rate passes through a maximum.

Corrosion rate and electrochemical noise resistance

As shown in Figure 4-6 a and b, under subcritical conditions, the corrosion rate of Type 304 SS is a linear function of flow rate, whereas, under supercritical conditions (Figure 4-7), the dependence of corrosion rate on flow rate deviates from linearity at the highest flow rate employed. However, for both subcritical and supercritical fluids, the inverse noise resistance is in good correlation with the corrosion rate.

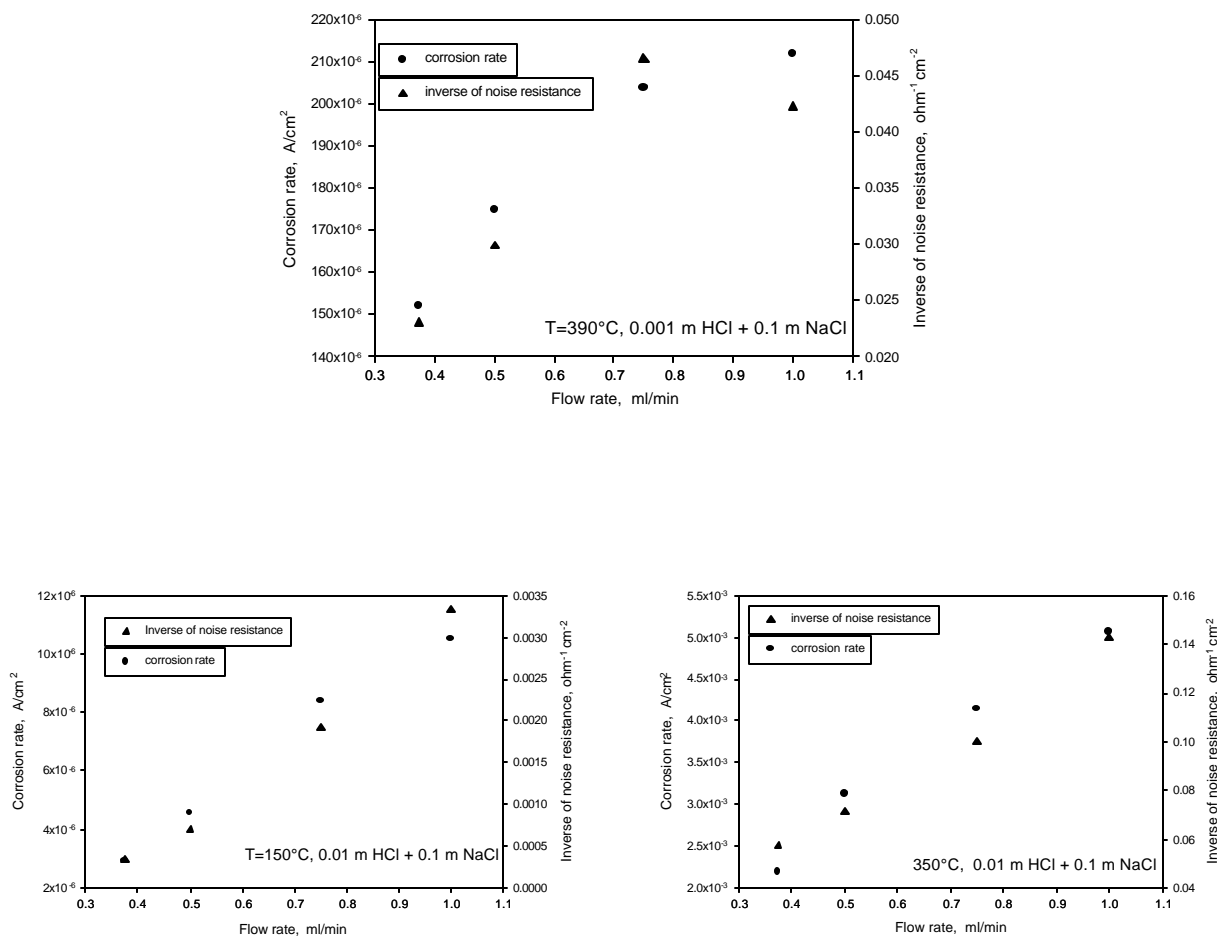


Figure 4-6. Inverse noise resistance and corrosion rate plotted as functions of flow rate for subcritical and supercritical temperatures.

Because the test solution was saturated with hydrogen, the cathodic reaction must be hydrogen evolution. At higher flow rate, the hydrogen bubbles were more readily flushed away from the surface and hence the cathodic reaction and the whole corrosion process are accelerated. The periodic detachment of hydrogen bubbles may also result in micro-transients of potential and current and hence have also been proposed as a source of electrochemical noises [21]. However, at least as observed under ambient conditions, this process apparently gives rise to relatively low frequency components in the noise spectrum, and it is unlikely that bubble detachment, the rate of which should also reflect the rate of the cathodic partial reaction and hence the corrosion rate, can account for the observed noise in totality.

The relationship between the corrosion rate and the inverse noise resistance is exhibited in Figure 4-7, where the logarithmic corrosion rate is plotted against the logarithmic inverse noise resistance. The results reveal that the corrosion rate is proportional to the inverse noise resistance at temperatures higher than 150°C.

Stern-Geary relationship

Because: 1) The reference electrode in the EN sensor, the Pt (H₂/H⁺) electrode, was stable and quiescent in the hydrogenated solution, 2) the instrumentation noise was negligible, 3) a low sampling frequency was used ($f_{\max} = 2$ Hz), and 4) the solution resistance was much lower than the electrode impedance [42], R_n should be equal to R_p , as indicated above.

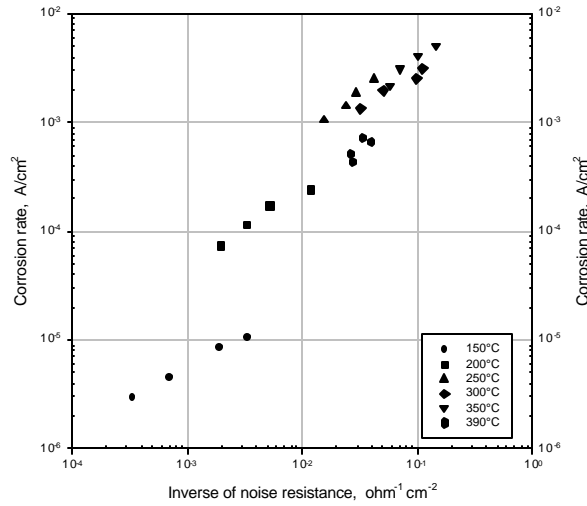


Figure 4-7. Relation between corrosion rate and inverse noise resistance.

Stern and Geary [43] proposed that if the corrosion potential and current were determined by the intersection of anodic and cathodic Tafel-type polarization curves, the Stern-Geary relationship (Eq. 2-2) must hold with the constant B being related to the anodic and cathodic Tafel constants by

$$B = \frac{b_a b_c}{2.303(b_a + b_c)} \quad (4-5)$$

where b_a and b_c are, respectively, the Tafel parameters for the anodic and cathodic reactions. However, Stern's work [43-46] has also shown that Eq. (4-5) does not always hold and that the coverage of the anodic/cathodic areas plays a critical part in this context. In a review, Gabrielli and Keddam [47] considered five different situations of corrosion: 1) Anodic and cathodic reactions are one step processes and are Tafelian electron transfer-controlled; 2) the anodic reaction is a one step process and is Tafelian electron transfer-controlled, but the cathodic reaction is purely diffusion controlled; 3) the anodic reaction is one step process and is Tafelian electron transfer-controlled, but the cathodic reaction is partly charge transfer- and partly diffusion-controlled; 4) both the anodic and cathodic reactions are irreversible, Tafelian multiple step processes; and 5) the electrode is in the passive state. Only for the first situation is the Stern-Geary constant expressed by Eq. (4-5).

Actually, the relation between the corrosion rate and the inverse polarization resistance or the inverse noise resistance can be derived by considering the Butler-Volmer equation [41,48]. Thus, for the anodic reaction (dissolution of metal), the following applies:

$$I_a = \frac{e^{\frac{2.303(E-E_{0,a})}{b_a}}}{\frac{1}{I_{0,a}} + \frac{1}{I_{l,a}} e^{\frac{2.303(E-E_{0,a})}{b_a}}} \quad (4-6)$$

and for the cathodic reaction (hydrogen evolution):

$$I_c = \frac{e^{\frac{-2.303(E-E_{0,c})}{b_c}}}{\frac{1}{I_{0,c}} - \frac{1}{I_{l,c}} e^{\frac{-2.303(E-E_{0,c})}{b_c}}} \quad (4-7)$$

where $I_{0,a}$ and $I_{0,c}$ are, respectively, the exchange current densities for the anodic and cathodic reactions, $E_{0,a}$ and $E_{0,c}$ are the corresponding equilibrium potentials, E is the electrode potential, and $I_{l,a}$ and $I_{l,c}$ are the limiting anodic and cathodic currents. Since, at realistic corrosion potentials, $I_{l,a} \gg I_{0,a}$, Eq. (4-6) can be simplified as:

$$I_a = I_{0,a} e^{\frac{2.303(E-E_{0,a})}{b_a}} \quad (4-8)$$

which is Tafelian in nature.

The behavior of $I_{l,c}$ is governed by the mass transport process, and can be related to the bulk hydrogen concentration (C_{H_2}) and the diffusivity of hydrogen (D_{H_2}) by:

$$I_{l,c} = \frac{nFC_{H_2}D_{H_2}}{\mathbf{d}} \quad (4-9)$$

where n is the number of electrons involved in the reaction, F is Faraday's constant, and \mathbf{d} is the effective (Nernst) diffusion layer thickness. For laminar flow conditions, the mass transfer coefficient ($K = \frac{D_{H_2}}{\mathbf{d}}$) can be expressed as:

$$K = 0.807 D_{H_2} \left(\frac{\mathbf{b}_l}{D_{H_2} L} \right)^{1/3} \quad (4-10)$$

where L is the length of the electrode and \mathbf{b}_l is the laminar velocity gradient on the electrode surface. \mathbf{b}_l is a linear function of the linear velocity u_l :

$$\mathbf{b}_l = Gu_l \quad (4-11)$$

and G is a geometric factor. Thus, the limiting cathodic current is a linear function of flow velocity.

The total external current (I) is an algebraic summation of the anodic and cathodic current and hence:

$$I = \mathbf{a}I_a - (1-\mathbf{a})I_c \quad (4-12)$$

where \mathbf{a} is the coverage of anodic region on the surface, which may be a function of potential, pH, and flow rate. Thus, for free corrosion conditions, we have:

$$I = 0 = \mathbf{a}I_{0,a} e^{\frac{2.303(E_{corr}-E_{0,a})}{b_a}} - (1-\mathbf{a}) \frac{e^{\frac{-2.303(E_{corr}-E_{0,c})}{b_c}}}{\frac{1}{I_{0,c}} - \frac{1}{I_{l,c}}} e^{\frac{-2.303(E_{corr}-E_{0,c})}{b_c}} \quad (4-13)$$

where E_{corr} is the corrosion potential. Accordingly, from the above relationship, we can derive the corrosion current (I_{corr}) as:

$$I_{corr} = \mathbf{a}I_{0,a} e^{\frac{2.303(E_{corr}-E_{0,a})}{b_a}} = (1-\mathbf{a}) \frac{e^{\frac{-2.303(E_{corr}-E_{0,c})}{b_c}}}{\frac{1}{I_{0,c}} - \frac{1}{I_{l,c}}} e^{\frac{-2.303(E_{corr}-E_{0,c})}{b_c}} \quad (4-14)$$

The linear polarization resistance is defined as:

$$\frac{1}{R_p} = \left(\frac{dI}{dE} \right)_{E=E_{corr}} \quad (4-15)$$

Thus, from Eqs. (4-12, 4-14, and 4-15),

$$\frac{1}{R_p} = I_{corr} \frac{1}{\mathbf{a}} \left(\frac{\partial \mathbf{a}}{\partial E} \right)_{E=E_{corr}} + I_{corr} \frac{2.303(b_a + b_c)}{b_a b_c} - I_{corr}^2 \frac{2.303}{b_c I_{l,c}} \quad (4-16)$$

Generally speaking, the inverse polarization resistance or noise resistance is not proportional to the corrosion current, but depends on potential, pH, and flow rate, especially when \mathbf{a} is not a constant with

respect to potential. However, when the first term on the right side of Eq. (4-16) is negligible, there are several cases where the inverse polarization resistance is proportional to corrosion current. They are as follows:

1. If the cathodic reaction is charge transfer controlled, i.e. $I_{l,c} \gg I_{corr}$,

$$\frac{1}{R_p} = I_{corr} \frac{2.303(b_a + b_c)}{b_a b_c} \quad (4-17)$$

which is exactly the Stern-Geary case.

2. If, however, the cathodic reaction is purely mass transport controlled, i.e. $I_{corr} = I_{l,c}$,

$$\frac{1}{R_p} = I_{corr} \frac{2.303}{b_a} \quad (4-18)$$

For both of the above cases, the ratio of R_p to I_{corr} does not depend on flow rate.

3. If the entire surface of the electrode is in the passive state and the anodic current is a constant with respect to potential (which is only true if the passive film is a cation interstitial or an oxygen ion conductor [51]):

$$\frac{1}{R_p} = I_{corr} \frac{2.303}{b_c} \quad (4-19)$$

For the above three cases, the ratio of the corrosion rate to the inverse noise resistance is a constant with respect to potential, pH, and flow rate. It is also clear that: 1) the Stern-Geary constant may not be related to the Tafel coefficients in the form of Eq. (4-5); 2) even the proportionality of inverse polarization resistance to corrosion rate may not exist; and 3) the dependence of the corrosion rate on inverse noise resistance may vary with temperature, pH, and flow rate.

Values of the limiting cathodic current for hydrogen evolution/oxidation at elevated temperatures have been determined previously by Macdonald et al [41] and by Biswas [48]. Comparison of the limiting cathodic current with the corrosion current, as evaluated from the mass loss tests carried out in the present study, suggests that the cathodic reaction is not mass transport controlled. In calculating the mass loss, we assumed that the corrosion current density remained constant over the entire experimental period. We regard this to be a reasonable approximation considering the active state within which the corrosion apparently occurs.

From Figure 4-7, it is clear that the corrosion rate is inversely proportional to the inverse noise resistance at temperatures higher than 150°C, whereas at 150°C the linear relationship between the corrosion rate and the inverse noise resistance is not observed. This non-proportionality may be due to the existence of partial passivity at 150°C. Thus, the non-proportionality may arise from the coverage of the anodic areas being a function of potential and flow rate, as shown by Eq. (4-16). Alternatively, since the corrosion rate in the passive areas is very small, we might underestimate the corrosion rate in the anodic areas when using Eq. (4-2), where A should be the area of the active region on the electrode surface instead of the total exposed area. Finally, we note that the lack of proportionality was observed at only a single temperature and we caution the reader not to read too much into this observation until it has been confirmed by additional experimentation.

Table 4-2. Stern Geary constant, B^* ($I_{corr}=B^*/R_n$), evaluated via ENA and B ($B=b_a b_c/(b_a+b_c)$) evaluated via polarization measurements.

Temperature °C	B^* (ENA), volts	b_c , volts	b_a , volts	B (polarization), volts
150	0.007	0.07	0.17	0.022
200	0.02	0.17	0.19	0.039
250	0.07	0.60	0.21	0.068
300	0.04	0.40	0.23	0.063
350	0.045	No data	No data	No data
390	0.008	No data	No data	No data

Electrochemical noise analysis and polarization measurement

Tafel coefficients for both metal dissolution and hydrogen evolution at elevated temperatures (up to 300°C) were determined by Huang et al [49] and by Macdonald et al. [41] via polarization measurements. The Stern-Geary constants evaluated from the Tafel coefficients using Eq. (4-5) and those evaluated from the regression of experimental data shown are present in Table 4-2. Because, strictly speaking, at 150°C, the ratio of the corrosion rate to the inverse noise resistance was observed not to be a constant, the value of the Stern-Geary constant for 150°C in Table 4-2 is actually an average of the ratios of the corrosion rate to the inverse

noise resistance. The discrepancy between the Stern-Geary constants evaluated by these two methods is a maximum of 68% for 150°C and is a minimum of 3% for 250°C.

References

1. J. Dobson, P. Snodin, and H. Thirsk, "EMF measurements of cells employing metal-metal oxide electrodes in aqueous chloride and sulfate electrolytes at temperatures between 25-250°C", *Electrochem. Acta*, Vol.21, pp.527-533, 1976.
2. D. Macdonald, P. Wentreck, and A. Scott, "The measurement of pH in aqueous systems at elevated temperatures using palladium hydride electrodes", *J. Electrochem. Soc.*, Vol.127, pp.1745-1751, 1980.
3. F.W. Sweeton, R.E. Mesmer, and C.F. Baes Jr., "A high temperature flowing EMF cell", *J. Phys. E6*, pp.165-168, 1973.
4. R.E. Mesmer, D.A. Palmer, and D.J. Wesolowski, "Potentiometric studies at ORNL with hydrogen electrode concentration cells" in *Physical Chemistry of Aqueous Systems: Meeting the Needs of Industry*, Begell House, New York, pp.423-431, 1995.
5. D.J. Wesolowski, D.A. Palmer, R.E. Mesmer, "Measurement and control of pH in hydrothermal solutions: in *Water-Rock Interaction*, Balkema, Rotterdam, pp.51-55, 1995.
6. L.W. Niedrach, "A new membrane-type pH sensor for use in high temperature-high pressure water", *J. Electrochem. Soc.*, Vol.127, pp.2122-2130, 1980.
7. L.W. Niedrach, W.H. Stoddard, "Development of a high temperature pH electrode for geothermal fluids", *J. Electrochem. Soc.* Vol.131, pp.1017-1026, 1984.
8. W.L. Bourcier, G.C. Ulmer, H.L. Barnes, "Hydrothermal pH sensors of ZrO₂, Pd hydrides and Ir oxides" in *Hydrothermal Experimental Techniques*, Wiley, New York, pp.158-188, 1987.
9. D.D. Macdonald, S. Hettiarachchi, and S. Lenhart, "The thermodynamic viability of yttria-stabilized pH sensors for high temperature aqueous solutions", *J. Solution Chem.*, Vol.17, pp.719-732, 1988.
10. D.D. Macdonald, S. Hettiarachchi, and H. Song, K. Mekela, R. Emerson, and M. Benhaim, "Measurement of pH in subcritical and supercritical aqueous systems", *J. Solution Chem.*, Vol.21, pp.849-881, 1992.
11. S.N. Lvov, G. Perboni, M. Broglia, "High temperature pH measurements in dilute aqueous ammonia solutions", in *Physical Chemistry of Aqueous Systems: Meeting the Needs of Industry*, Begell House, New York, pp.441-448, 1995.
12. K. Ding, W.E. Seyfried, "Direct pH measurement of NaCl-bearing fluid with in situ sensor at 400°C and 40 megapascals", *Science*, Vol.272, pp.1634-1635, 1996.
13. S.N. Lvov, H. Gao, D.D. Macdonald, "Advanced flow-through external pressure-balanced reference electrode for potentiometric and pH studies in high temperature aqueous solutions", *J. Electroanal. Chem.*, Vol.443, pp.186-190, 1998.
14. S.N. Lvov, H. Gao, D.Kouznetsov, I. Balachov and D.D. Macdonald, "Potentiometric pH measurements in high subcritical and supercritical aqueous solutions", *Fluid Phase Equilibria*, Vol.150/151, pp.515-520, 1998.
15. S.N. Lvov, X.Y. Zhou, D.D. Macdonald, "Flow-through electrochemical cell for accurate pH measurements to 400°C", *J. Electroanal. Chem.*, Vol.463, pp.146-156, 1999.
16. L. B. Kriksunov and D. D. Macdonald, Proc. 12th International Conference on the Properties of Water and Steam, Orlando FL, Sept. 1994, Begell House, (1995).
17. T. Hegyard, J.R. Williams, *Trans. Faraday Soc.*, 57(1961): p. 2288.
18. Inverson, *J. Electrochem. Soc.*, 115(1968): p. 617.
19. K. Hladkey, J. Dawson, *Corr. Sci.*, 22(1981): p. 317.
20. K. Hladkey, J. Dawson, *Corr. Sci.*, 23(1982): p. 231.
21. J. Dawson, "Electrochemical Noise Measurement: The Definitive In-situ Technique for corrosion applications?", *ASTM STP 1277*, 1996, p. 3.
22. D.A. Eden, M. Hoffman, and B.S. Skerry, *Polymeric Materials for Corrosion Control*, ACS Symposium Series, vol. 322, ACS, 1986, p. 36.
23. C-T. Chen, B.S. Skerry, *Corrosion*, 47(1991): p. 598.
24. F. Mansfeld, H. Xiao, *J. Electrochem. Soc.*, 140(1993): p. 2205.
25. H. Xiao, F. Mansfeld, *J. Electrochem. Soc.*, 141(1994): p.2332.
26. H. Xiao, L.T. Han, C.C. Lee, and F. Mansfeld, *Corrosion*, 53(1997): p. 412.
27. F. Mansfeld, C.C. Lee, *J. Electrochem. Soc.*, 144(1997): p. 2068.
28. U. Bertocci, C. Gabrielli, F. Huet, M. Keddam, and P. Rousseau, *J. Electrochem. Soc.*, 144(1997): p. 37.
29. G. Gusmano, G. Montesperelli, S. Pacetti, and A. D'Amico, *Corrosion*, 53(1997): p. 860.
30. U. Bertocci, C. Gabrielli, F. Huet, and M. Keddam, *J. Electrochem. Soc.*, 144(1997): p. 31.
31. U. Bertocci, F. Huet, *J. Electrochem. Soc.*, 144(1997): p. 2786.

32. C. Liu, D.D. Macdonald, E. Medina, J.J. Villa, and J.M. Bueno, *Corrosion*, 50(1994): p. 687.
33. D.D. Macdonald, C. Liu, and M.P. Michael, "Electrochemical Noise Measurements on Carbon and Stainless Steel in High Subcritical and Supercritical Aqueous Environments", *ASTM STP 1277*, 1996, p. 247.
34. X.Y. Zhou, S.N. Lvov, S.M. Ulyanov, "Safety Yttria-Stabilized Zirconia (YSZ) pH Sensing Electrode for High Temperature Aqueous Systems", US Patent Application (submitted).
35. D. Tsuruta, D.D. Macdonald, "Measurement of pH and potential in boric acid/lithium hydroxide buffer solutions at elevated temperatures", *J. Electrochem. Soc.* **128**, (1981) 1199-1203.
36. K. Eklund, S.N. Lvov, and D.D. Macdonald, "The measurements of Henry's constant for hydrogen in high subcritical and supercritical aqueous systems", *J. Electroanal. Chem.* **437**, (1997) 99-110.
37. R.A. Robinson, R.H. Stokes, *Electrolyte Solutions*, Butterworths Scientific, 1959.
38. I. Mills, T. Cvitas, K. Homann, N. Kallay, and K. Kuchitsu, *Quantities, Units and Symbols in Physical Chemistry*, Blackwell, Oxford, 1993, pp.60-62.
39. X.Y. Zhou, A. Bandura, S.M. Ulyanov, S.N. Lvov, "Calculation of Diffusion potentials in Aqueous Solutions Containing HCl, NaCl and NaOH at Temperatures from 25 to 400°C", 13rd Inter. Conf. on Properties of Water and Steam, Spet. 12-16, 1999, Toronto, Canada.
40. I. Olefjord, B. Brox, "Quantitative ESCA Analysis of the Passive State of an Fe-Cr Alloy and an Fe-Cr-Mo Alloy", Passivity of Metals and Semiconductors, Proceedings of the Fifth International Symposium on Passivity, Bombannes, France, Elsevier Science Publishers, 1983, p. 561.
41. D.D. Macdonald, S.N. Lvov, G. Kelkar, J.F. Magalhaes, H-S. Kwon, A. Wuensche, R. Biswas, Z. Ahmad, and G. Englehardt, "The Development of Deterministic Methods for Predicting Corrosion Damage in Water Cooled Nuclear Reactors", ESEERCO Report EP93-33, 1996.
42. X. Zhou, X.J. Wei, S.N. Lvov, and D.D. Macdonald, "Evaluation of Corrosion Rate of Type 304 SS in Subcritical and Supercritical Aqueous Solutions by Polarization, AC Impedance, and Electrochemical Noise Techniques", in preparation.
43. M. Stern, A.L. Geary, *J. Electrochem. Soc.*, 104(1957): p. 56.
44. M. Stern, R.M. Roth, *J. Electrochem. Soc.*, 104(1957): p. 390.
45. M. Stern, *J. Electrochem. Soc.*, 104(1957): p. 559.
46. M. Stern, *J. Electrochem. Soc.*, 104(1957): p. 645.
47. C. Gabrielli, M. Keddam, *Corrosion*, 48(1992): p. 794.
48. R. Biswas, "Investigation of Electrochemical Phenomena in High Temperature Aqueous Systems", Ph. D. Thesis, Pennsylvania State University, 1999.
49. S. Huang, K. Daehling, T.E. Carleson, M. Abdel-Latif, P. Taylor, C. Wei, and A. Propp, "Electrochemical Measurements of Corrosion of Iron Alloys in Supercritical Water", *Supercritical Fluid Science and Technology*, ACS, 1988, p. 287.
50. L. Kriksunov and D. D. Macdonald, *J. Electrochem. Soc.*, "Corrosion in Supercritical Water Oxidation Systems: A Phenomenological Analysis", *J. Electrochem. Soc.*, 142 (1995), p. 4069.
51. D. D. Macdonald, "Passivity – the key to our metals-based civilization", *Pure Appl. Chem.*, 71 (1999), p. 951.

5. Effect of Pressure on Corrosion Rate

During the course of this study, the PI (Prof. Digby Macdonald), who also acted as a consultant to a contractor (Stone & Webster Engineering Corp) on the development of SCWO for the destruction of chemical weapons (VX) hydrolysate, was asked to analyze the impact of pressure on some MOC (Materials of Construction) corrosion experiments that were being performed in another university laboratory. The experiments were being performed on candidate structural and liner materials (Ni 201, Pt, and Pt/C-276 weldments) for use in SCWO reactors. These experiments were designed to provide information of an engineering nature on the rate and form of attack. However, difficulties in controlling the pressure at the target value of 3500 ± 250 psi (238.2 ± 17 bar) resulted in pressure excursions as high as 4025 psi (273.9 bar) and as low as 2600 psi (177 bar). The objective of the analysis was to explore the impact of pressure on the corrosion rate, in order to ascertain the impact of the pressure excursions on the observed corrosion damage. Because of the dearth of information on the effect of pressure on the rates of corrosion processes in high subcritical and supercritical aqueous systems, the calculations presented in this report are based upon theoretical principles, augmented where possible by experimental information. The work has been included in the present report, because it represents, to the authors' knowledge, the first critical analysis of the effect of pressure on the rate of corrosion of metals and alloys in supercritical aqueous media. Our previous theoretical work [1] work

emphasized the effect of temperature on the corrosion rate and it successfully predicted the maximum in corrosion rate at high subcritical temperatures, as discussed above.

The corrosion of metals and alloys in high subcritical aqueous systems, and especially in supercritical environments, displays characteristics that place the system between an ionically conductive phase, such as an electrolyte solution at ambient temperature, and a gas [1]. Processes involving ions, which exist because the solvent has a high dielectric constant (see below), dominate corrosion processes in aqueous solutions under ambient conditions. On the other hand, corrosion in the gas phase (excluding plasmas) is dominated by molecular processes, such as the direct reaction of the metal with oxygen and/or water. The reaction rate may range over many orders in magnitude in either case, depending upon the characteristics of the system, as the conditions (including pressure) are varied. However, the origin of the effect of pressure on reaction rate depends upon the properties of the environment and on the activation process.

The rate (R) of a corrosion process, such as the corrosion of a metal in an oxygenated acidic solution, can be written in chemical reaction terms as

$$R = k(C_{O_2})^n (C_{H^+})^m \quad (5-1)$$

where k is the rate constant, C_{O_2} and C_{H^+} are the volumetric (molar) concentrations of oxygen and hydrogen ion, respectively, and n and m are the corresponding reaction orders. Because the concentrations are volumetrically based, their values depend upon the density and hence upon the pressure. Additionally, the rate constant, k , is pressure dependent, because the activated complex (the “transition state”) has a different volume from that of the initial state (metal + O_2 + H^+), as discussed below. Finally, a change in pressure will also affect the degree of dissociation of acids, bases, and salts, primarily through the effect of pressure on the dielectric constant and density of the medium. This, in turn, will result in the concentration of H^+ in Equation (5-1) being pressure dependent. Thus, the effect of pressure on the rate of a reaction can be delineated into three separate effects; an effect on the free energy of activation, an effect on the volumetric concentrations of the reactants, and an effect on the dissociation of acids, bases, and salts. Each of these effects is considered below.

Theoretical Principles

Prior to developing the theoretical principles upon which these calculations are based, it is important to comment on the form of Equation (5-1). As noted above, the equation is written in a form that is commonly employed for homogeneous reactions, whereas corrosion reactions are heterogeneous reactions. Indeed, corrosion reactions may be decomposed into partial anodic and cathodic charge transfer reactions (e.g. $M \rightarrow M^{2+} + 2e^-$ and $\frac{1}{2} O_2 + 2H^+ + 2e^- \rightarrow H_2O$). The Wagner-Traud hypothesis states that, under freely corroding conditions, the rates of the two partial reactions are equal, so that no net accumulation of charge occurs. Thus, the addition of the two partial reactions yields $M + \frac{1}{2} O_2 + 2H^+ \rightarrow M^{2+} + H_2O$, which is formally indistinguishable from a chemical reaction. Accordingly, the form of Equation (5-1) is justified.

The molar concentration of a species can be expressed in terms of the masses of the components in the system and the density as follows:

$$C = 1000 \cdot \rho \cdot W_s / M_s \cdot (W_s + W_{H_2O}) \quad (5-2)$$

where ρ is the density (g/cm^3), M_s is the molecular weight of the solute (g/mol), and W_s and W_{H_2O} are the masses of the solute and solvent (H_2O), respectively, in the system. Only the density in this equation is pressure dependent and by differentiation of the natural log of both sides we obtain

$$[\partial \ln(C) / \partial P]_T = [\partial \ln(\rho) / \partial P]_T = \kappa \quad (5-3)$$

where κ is the compressibility of the system

$$\kappa = -(\partial V / \partial P)_T / V. \quad (5-4)$$

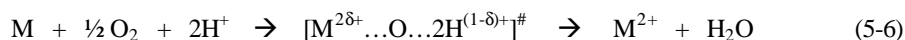
For relatively dilute solutions, the compressibility may be taken as that for pure water, which is available from the steam tables.

Activated complex theory shows that the pressure dependence of the rate constant, k , can be expressed as

$$[\partial \ln(k)/\partial P]_T = -\Delta V^\ddagger / R_g \cdot T \quad (5-5)$$

where ΔV^\ddagger (cm^3/mol) is the volume of activation for the reaction, R_g is the universal gas constant ($R_g = 82.05 \text{ atm}\cdot\text{cm}^3/\text{K}\cdot\text{mol}$), and T is the absolute temperature. The form of Equation (5-5) is such that if ΔV^\ddagger is positive, increasing pressure decreases the rate constant and hence inhibits the reaction from occurring. On the other hand, if ΔV^\ddagger is negative, increasing pressure increase the rate constant and hence accelerates the reaction. In a sense, Equation (5-1), describes a “kinetic LeChatelier Principle”, in that the system moves in the direction so as to relieve the effects of an environmental stress (in this case, a change in pressure).

The particular reaction of interest may be written for illustrative purposes as



where M is the metal, the entity in square brackets is the activated complex (the “transition state”), and δ is the extent of charge transfer at the knoll in the reaction coordinate between the initial state (left side) and the final state (right side). Note that when $\delta = 0$, the system is in the initial state, but when $\delta = 1$ it is in the final state. The exact location of the transition state can only be determined by detailed quantum mechanical calculations, which are well beyond the scope of the present analysis. Instead, it is sufficient to note that δ may be taken as 0.5, to a good approximation. It is also important to note that the total charge on the transition state is the same as those on the initial state and the final state. That is, the reaction is *isocoulombic*. This observation is important, because it suggests that the contribution to ΔV^\ddagger from electrostriction is small. The concept employed above for viewing the transition state is termed the *partial charge method*, which has been used extensively to describe charge transfer reactions at interfaces.

Further insight into the volume of activation may be gained by writing ΔV^\ddagger in terms of the partial molar volumes of the entities that are involved in the activation process, viz.

$$\Delta V^\ddagger = V^\ddagger - V_M - \frac{1}{2} V_{O_2} - 2V_{H^+} \quad (5-7)$$

where V^\ddagger , V_M , V_{O_2} , and V_{H^+} are the partial molar volumes of the transition state, the metal, oxygen, and the hydrogen ion, respectively. If the volume of activation is known, from measurements of the pressure dependence of the rate constant, and noting that the partial molar volumes of the initial state components are readily determined, it is possible to estimate the partial molar volume of the transition state. Comparison of this value with those for model compounds allows one to estimate the extent of charge development in the transition state. This has been done for chemical reactions, for example for the hydrolysis of benzyl chloride [2], but not for corrosion reactions, to the authors’ knowledge. Nevertheless, the theory outlined above is equally applicable to corrosion reactions as it is to any other reaction.

Returning now to Eq. (5-1) and taking natural logarithms of both sides, followed by differentiation with respect to pressure, yields the pressure dependence of the reaction rate as

$$[\partial \ln(R)/\partial P]_T = -\Delta V^\ddagger / R_g \cdot T + (n + m) \cdot \kappa \quad (5-8)$$

in which only the first two effects are considered. Using the method of small differences, and by adding a term for the third effect (dissociation of the acid), we can now estimate the impact of a small change in pressure from P_0 to P on the reaction rate. The expression obtained from Eq. (5-8) with HCl dissociation added is given by:

$$\ln(R/R_0) \approx (-\Delta V^\ddagger / R_g \cdot T) \cdot (P - P_0) + (n + m) \cdot \kappa \cdot (P - P_0) + n \cdot \ln[C_{H^+}(P) / C_{H^+}(P_0)] \quad (5-9)$$

The first term in Eq. (5-9) is due to the effect of pressure on the free energy of activation, while the second term arises from the effect of pressure on the volumetric concentrations of the reactants (O_2 and H^+). The third term describes the effect of pressure on the dissociation of HCl in the environment, where $C_{H^+}(P)$ is the molar concentration of H^+ at the pressure P . Note that, in deriving Eq. (5-9), no assumptions were made with respect to the state of the system, so that it is equally applicable to the subcritical state as it is to the supercritical state.

We now apply the theory developed above to corrosion reactions that occur within aqueous systems at high subcritical and low supercritical temperatures, so as to capture the essential features of the experiments. While we do not have experimentally measured values for ΔV^\ddagger for any corrosion reaction, we may make a reasonable estimate of the value of this quantity from the nature of the reaction. Thus, as noted earlier, the reaction is isocoulombic in forming the transition state, which means that the electrostrictive component

should be small. Because the charge is spread over a larger surface in the transition state than it is in the initial state, the electrostrictive component is probably negative (i.e. water will be drawn into the transition state by ion-dipole interaction). Furthermore, because the transition state involves the coming together of several entities, the structural contribution to ΔV^\ddagger is also likely to be negative. Accordingly, the volume of activation, as a whole, is estimated to be negative. Now, chemical reactions generally exhibit volumes of activation that lie within $\pm 50 \text{ cm}^3/\text{mol}$ (e.g. that for the hydrolysis of benzyl chloride in water is about $-10 \text{ cm}^3/\text{mol}$. [2]). Accordingly, as a conservative position, an activation volume of $-50 \text{ cm}^3/\text{mol}$. is selected for the following analysis.

The kinetic orders of the corrosion reaction with respect to O_2 and H^+ are not known for the particular system of interest. However, the order with respect to oxygen may be taken as $n = 0.5$, corresponding to the initial dissociation of O_2 onto the metal surface. This value agrees with the experimentally measured kinetic order with respect to oxygen for the corrosion of carbon steel in high subcritical oxygenated water, as reported by Liu et. al. [3]. Again, no data are available for the kinetic order of the particular corrosion process of interest with respect to H^+ , and none could be found for any other reaction under the relevant conditions. Accordingly, it is assumed that the reaction is first order and hence that $m = 1$.

The compressibility, density, viscosity, and dielectric constant data used in these calculations were taken from the NIST Steam Algorithm [4] and correspond to those for pure water. It is assumed that, for the purposes of these scoping calculations, the values are also applicable to the hydrolysate. Finally, the effect of pressure on the composition of a dilute HCl solution was calculated using a model and algorithm (SuperCrit_pH) developed by the PI a number of years ago for simulating the chemical properties of high subcritical and supercritical aqueous systems.

The hydrolysate used in the experiments is a complex mixture of inorganic and organic chemicals and the requisite thermodynamic data are not available to model the input solution accurately. However, the organic compounds are oxidized rapidly, so that the solution quickly becomes an inorganic system containing phosphate, sulfate, nitrate, and chloride ions. It is further assumed that the system is effectively neutralized by the added sodium hydroxide. Accordingly, it is assumed that the activity of hydrogen ion is determined by the dissociation of HCl in the system. This is obviously a gross over-simplification but, to the author's knowledge, an effective chemical model for fully hydrolyzed hydrolysate has not yet been developed. Development of such a model remains as a pressing need in the development of SCWO technology for the destruction of chemical agents.

In simulating the effect of positive excursions in pressure, a pressure increase of 35.72 bar has been assumed, corresponding to a maximum pressure of 4025 psi. The results of these calculations are summarized in the following table:

Table 5-1. Estimated Influence of Pressure on the Rate of Corrosion for a Positive Pressure Excursion from 3500 psi (238.16 b) to 4025 psi (273.88 b).

Zone	Temperature ($^\circ\text{C}$)	P_0 (b)	ΔP (b)	R/R_0
1. Subcritical	343.3	238.2(3500 psi)	35.72	1.095
2. Subcritical	371.1	238.2(3500 psi)	35.72	1.622
3. Subcritical	365.5	238.2(3500 psi)	35.72	1.302

Also of interest is the impact of pressure on the three contributing terms given on the right side of Eq. (5-9). These contributions are shown in Table 5-2. As shown in Table 5-1, the predicted impact of pressure on the corrosion rate at the lowest temperature (Zone 1) is modest (less than 10 %) and the contributions from activation, density, and HCl dissociation [corresponding to the first, second and third terms, respectively, on the right side of Equation (9)] are roughly equal. At the highest temperature (Zone 3, Pt/C-276), which is only 4 $^\circ\text{C}$ below the critical temperature of water, the predicted impact of pressure on the corrosion rate is substantial, corresponding to an increase in the rate of more than 60 % for a pressure increase of 35.72 bar (525 psi). In this case (Table 5-2), the pressure dependence of the rate is dominated by HCl dissociation followed by density (volumetric concentration). The same is apparent for the intermediate temperature (Zone 3, Pt). The increasingly dominant roles played by the density (volumetric concentration) and HCl dissociation terms as the temperature is increased correspond to sharp decreases in the density and dielectric constant, and to an increase in the compressibility, as the temperature approaches the critical value.

The calculations have also been carried out for negative pressure excursions from the target pressure of 3500 psi (238.2 b) to the lower of 2600 psi (176.9 b). The results are summarized in Tables 5-3 and 5-4. For the lowest temperature (343.3 $^\circ\text{C}$), the predicted decrease in the reaction rate is not remarkable, being of the order of 16 %. Furthermore, approximately equal contributions are obtained from the activation, density (volumetric concentration), and HCl dissociation terms. On the other hand, very large decreases in the rate,

which are overwhelmingly dominated by HCl dissociation, are predicted for the two highest temperatures upon decreasing the pressure from 3500 psi to 2600 psi.

Table 5-2. Estimated Contributions of Activation, Density, and HCl Dissociation to the Change in Corrosion Rate for a Positive Pressure Excursion of 35.72 b (525 psi) from 3500 psi (238.16 b) to 4025 psi (273.88 b).

Zone	Activation	Density	HCl Dissociation	ln (R/R ₀)
1. Subcritical	0.0353	0.0305	0.025	0.091
3. Subcritical	0.0353	0.157	0.293	0.484
3. Subcritical	0.0353	0.090	0.140	0.264

Table 5-3. Estimated Influence of Pressure on the Rate of Corrosion for a Negative Pressure Excursion from 3500 psi (238.16 b) to 2600 psi (176.9 b)

Zone	Temperature (°C)	P ₀ (b)	ΔP (b)	R/R ₀
1 Ni 201	343.3	238.2(3500 psi)	-61.24	0.840
3 Pt/C-276	371.1	238.2(3500 psi)	-61.24	2.30x10 ⁻⁶
3 Pt	365.5	238.2(3500 psi)	-61.24	3.39x10 ⁻⁶

Under the low-pressure conditions, the dissociation constants for HCl and water are exceedingly low and hence so is the activity of hydrogen ion. A reduction in the corrosion rate by a factor of a million is judged to be unrealistic, because other corrosion reactions probably come into play, such as the reaction of the alloy with water, when the hydrogen ion activity is so low. Accordingly, it is considered that the most that should be read into the calculations for the two highest temperatures shown in Tables 5-3 and 5-4 is that the corrosion rates are “sharply reduced” upon reducing the pressure.

Table 5-4. Estimated Contributions of Activation, Density, and HCl Dissociation to the Change in Corrosion Rate for a Negative Pressure Excursion from 3500 psi (238.16 b) to 2600 psi (176.9 b).

Zone	Activation	Density	HCl Dissociation	ln (R/R ₀)
1 Ni 201	-0.0605	-0.0524	-0.0616	-0.175
3 Pt/C-276	-0.0579	-0.2691	-12.654	-12.981
3 Pt	-0.0584	-0.1543	-12.382	-12.594

The remaining question that we explore in this work is: “How realistic are the calculations?” The answer to this question was explored by repeating the calculations for the only experiment, of which the author is aware, in which the effect of pressure on the rate of a corrosion reaction at a super critical temperature has been explored in a quantitative and systematic manner. Thus, Liu, et. al. [3] measured the corrosion “activity” as the RMS of the noise in the coupling current between two identical Type 1013 carbon steel electrodes exposed to oxygenated water (0.006 ppm) at 481 °C. This system is clearly supercritical but, as noted elsewhere, the theory developed above makes no assumption as to the state of the system and hence is equally applicable to subcritical and supercritical solutions. The data employed in these calculations are given in Ref. 3 and the results of the calculations are summarized in Table 5-5. The calculated relative corrosion rate is compared with the measured values in Figure 5-1.

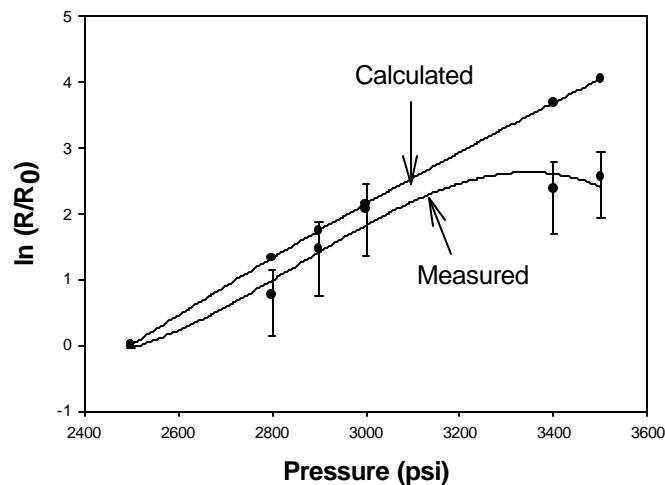


Figure 5-1. Plot of calculated relative reaction rate versus measured relative reaction rate for the corrosion of 1013 carbon steel in supercritical water at 481 °C.

The assumption that is made in this comparison is that the corrosion rate is proportional to the RMS of the noise in the coupling current. At the current time, there is no experimental or theoretical justification of this assumption, other than “it seems to work”. Examination of Figure 5-1 shows that the model is in remarkable agreement with the experimental data, particularly for low-pressure excursions. Note that in these calculations, there are no adjustable parameters, so that the comparison given in Figure 5-1 is a particularly robust test of the model. The deviations between theory and experiment observed at high pressures possibly arise from the assumed linearity inherent in the method of small differences. Nevertheless, the high level of agreement provides considerable confidence that the analysis reported in this study of the effect of pressure excursions on reaction rate is reasonably accurate.

Finally, it is necessary to comment on the relative importance of the three fundamental contributions to the relative corrosion rate for carbon steel in oxygenated, super critical water. The contributions are summarized in Table 5-5. As seen from this table, the activation contribution is of relatively lower importance compared with the contribution from HCl dissociation, when the temperature is increased from a high subcritical value (Table 5-2) to supercritical values (Table 5-3). Indeed, the effect of pressure on the reaction rate can be ascribed almost totally, in the case of the supercritical systems, to environmental effects. This property is characteristic of a “gas phase” reaction system, and it illustrates the profound changes that occur in kinetic processes upon transitioning the critical point in aqueous systems.

Table 5-5. Contributions of Activation, Density (Volumetric Concentration), and HCl Dissociation to the Effect of Pressure on the Corrosion of Type 1013 Carbon Steel in Oxygenated Water at 481 °C.

Pressure (psi)	Activation	Density	HCl Dissociation	(R/R ₀)
2500	0	0	0	1
2800	0.0165	0.2025	1.106	3.76
2900	0.0212	0.2640	1.457	5.71
3000	0.0275	0.3225	1.802	8.60
3400	0.0495	0.540	3.101	40.07
3500	0.0550	0.5850	3.411	57.45

References

1. L. B. Kriksunov and D. D. Macdonald, *J. Electrochem. Soc.*, **142**, 4069 (1995).
2. D. D. Macdonald and J. B. Hyne, *Can. J. Chem.*, **48**, 2494 (1970).
3. C. Liu, D. D. Macdonald, E. Medina, J. J. Villa, and J. M. Bueno, *Corrosion*, **50**, 687 (1994).
4. National Institute of Science and Technology, Gaithersburg, MD (1994).

6. Standardization of pH

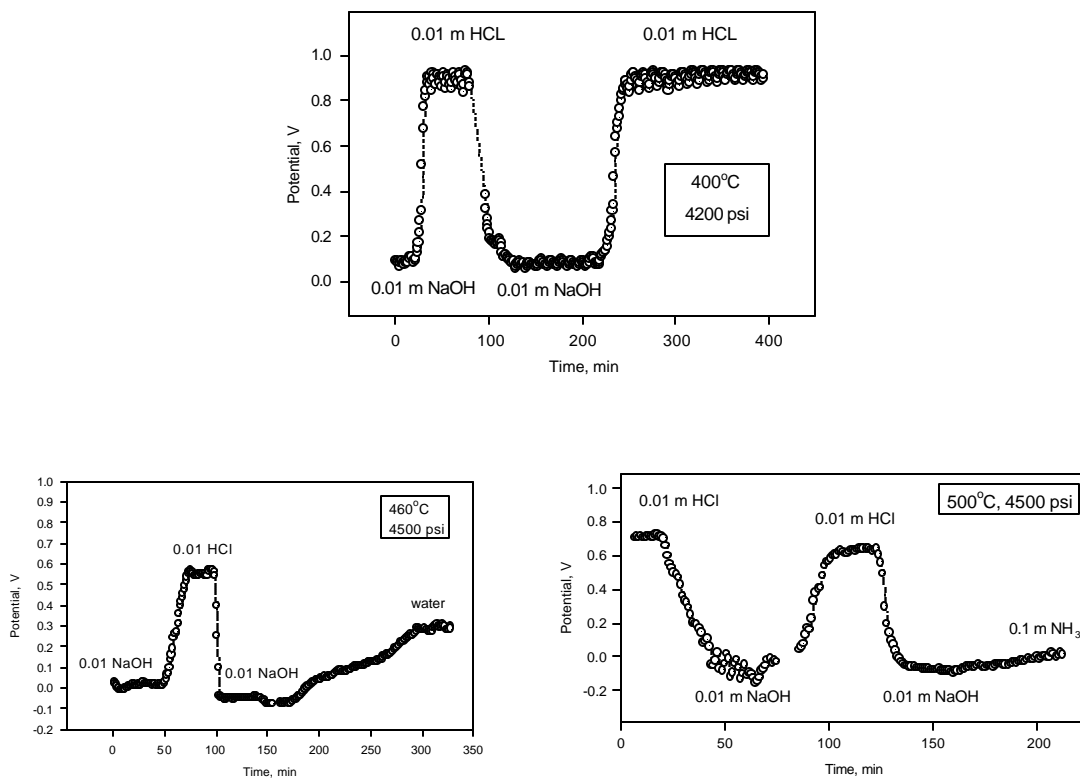
Knowledge of the pH of a solution at temperatures above the critical temperature (374°C for pure water) is of particular importance for numerous industrial applications, in particular for the destruction of organic waste using Supercritical Water Oxidation (SCWO) and for the operation of supercritical power plants. Many fundamental problems of high temperature aqueous chemistry, as well, are closely connected with the activity of hydrogen ions in the solution. Here, we propose the development of a standard scale for pH in supercritical aqueous systems, and we discuss the importance of knowing the activity of water when estimating the pH.

Measurements of pH

In a previous study [1], we employed YSZ (Ytria-Stabilized Zirconia) ceramic membrane pH sensors and External Pressure Balanced Reference Electrodes (EPBRE) to directly measure the pH of aqueous solutions at temperatures up to 530°C in a high temperature test cell analogous to that described Refs. 2-4. The internal reference element in the YSZ electrode was solid state Ag/AgCl, while the EPBRE was Ag/AgCl in saturated KCl at ambient temperature. The electrolyte bridge of the EPBRE (made of high density alumina) was filled with the autoclave solution and extended into the supercritical region of the HTHP test cell, terminating in the vicinity of the YSZ electrode.

In Figure (6-1), we present typical potentiometric data for the cell YSZ/EPBRE measured at temperatures of 400, 460, 500, and 525-528°C on cycling the input solution between acidic and basic conditions.

YSZ vs EPBRE (Ag/AgCl, sat. KCl)



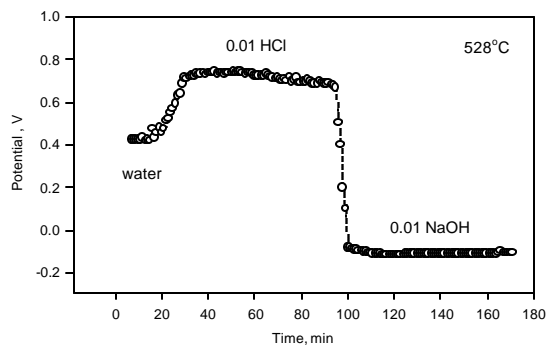


Figure 6-1. Potentials for the cell YSZ/EPBRE in response to cyclical acid and base injection at temperatures of 400, 460, 500, and 528 °C. Additional experimental details are given in Ref. 1.

Note that the estimated error in the measured cell potential is ± 30 mV, corresponding to an uncertainty in pH at the highest temperature of ± 0.2 . Accordingly, these data are not of the quality of those reported earlier in this report, but they have been measured at considerably higher temperatures

In Figure 6-2 we present results that were previously obtained [1] of an experiment in which a model, halogenated waste compound (CCl_4) was used to demonstrate the viability of pH measurement techniques being used for on-line monitoring in SCWO systems.

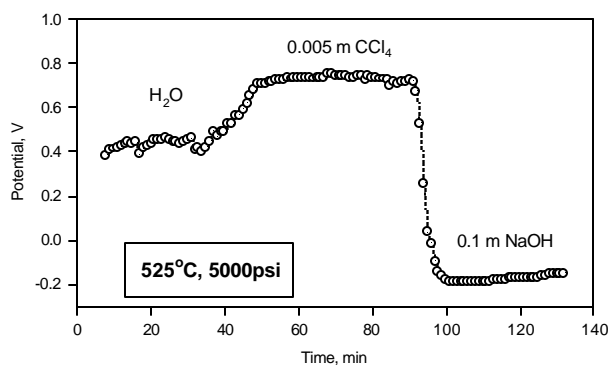
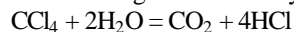


Figure 6-2. YSZ/EPBRE cell potential as a function of time upon the injection of 0.005 m carbon tetrachloride and subsequently the injection of 0.1 NaOH.

In the initial phase of the experiment, pure water was pumped through the reactor at 5000 psi and 525°C. We then introduced a solution of approx. 0.005 m CCl_4 . The pH of the solution indicated an immediate response and changed with time in the direction of a lower pH value (high cell potentials in the Figure 6-2). Clearly, carbon tetrachloride undergoes thermal hydrolysis, presumably according to the reaction:



We do not take into account reactions involving oxygen, because the concentration of oxygen in the air-saturated solution employed (approx. 7 ppm $\approx 0.0002\text{m}$) is much lower than the concentration of CCl_4 (0.005 m). Hence oxygen is not expected to significantly contribute to the decomposition of the model waste compound. The importance of the data shown in Figures 6-1 and 6-2 lies not only in the temperature at which they were measured but also in the fact that the YSZ sensor may be used to monitor the destruction of resilient organic compounds in aqueous solutions at supercritical temperatures.

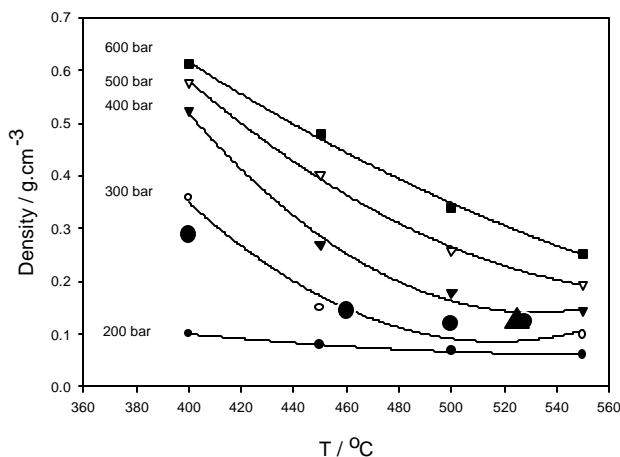


Figure 6-3. Plots of density versus temperature for supercritical water as a function of pressure. Also shown are the conditions for the pH measurements reported in Figures 6-1 (filled circles) and 6-2 (filled triangle).

It is also fruitful to explore the conditions under which the measurements reported in Figures 6-1 and 6-2 were actually made. Thus, we show in Figure 6-3, 6-4, and 6-5 plots of density, dielectric constant, and viscosity, respectively, versus temperature for pressures ranging from 200 bar to 600 bar. Superimposed on this diagram are the conditions that correspond to the measurements shown in Figures 61 and 62. Importantly, these data show that potentiometric measurements can be made not only at prototypical SCWO temperatures but also at densities, dielectric constants, and viscosities as low as 0.13 g/cm^3 , 2, and 0.033 cP, respectively. These conditions are more typical of a dense gas than they are of a liquid.

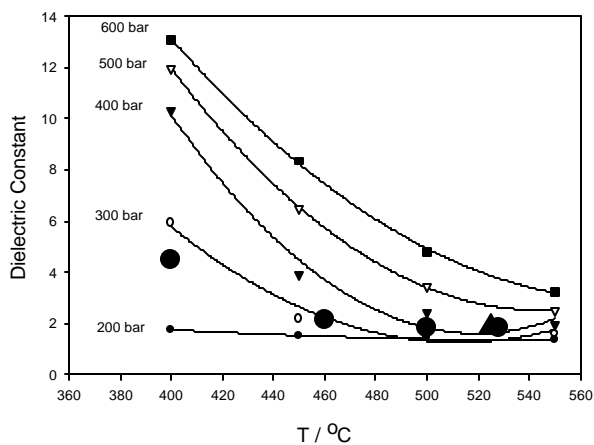


Figure 6-4. Plots of dielectric constant versus temperature for supercritical water as a function of pressure. Also shown are the conditions for the pH measurements reported in Figures 6-1 (filled circles) and 6-2 (filled triangle).

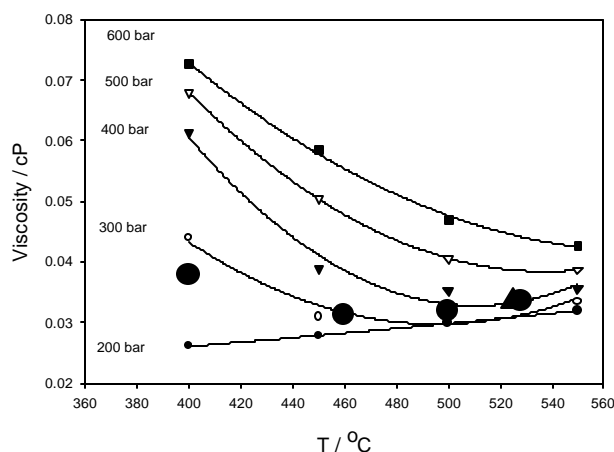


Figure 6-5. Plots of viscosity versus temperature for supercritical water as a function of pressure. Also shown are the conditions for the pH measurements reported in Figures 6-1 (filled circles) and 6-2 (filled triangle).

pH Standards

The pH scale for supercritical aqueous systems has not been defined at the present time. Standardization of the pH scale for supercritical systems, analogous to that for subcritical solutions, must be based upon somewhat arbitrary model assumptions and standard solutions. The unambiguous choice of standard solutions for supercritical aqueous systems is more complicated than that at subcritical temperatures, because of the poor dissociation of even strong electrolytes at $T > T_c$ and the relatively low values for activity coefficients. Experimental data for determining those parameters are scarce. Additional problems arise from the fact that many fundamental properties of high subcritical and supercritical aqueous solutions are strongly pressure-dependent. In this regard, aqueous solutions at the same temperature, but at significantly different pressures, should be considered as different systems, thereby greatly complicating the specification of pH standards. The problem is even further complicated by the pressure dependencies of the potential of the reference electrode, the thermal diffusion liquid junction (TDLJ) potential, and the liquid junction (LJ) potential.

To overcome these difficulties, we propose to define the pH scale for supercritical systems somewhat arbitrarily, based on available estimates of dissociation constants (K_d) and activity coefficients (γ) for solution of HCl, a common 1-1 electrolyte. The concentration of the solutions should be chosen to be reasonably low, to allow for complete solubility and reliable model estimates of K_d and γ , but at the same time should be much higher than the concentration of potential impurities and corrosion products in high temperature water. An additional advantage of using HCl is that this is a gaseous compound, so we should not expect significant problems with solubility and/or phase separation in the HCl solution in supercritical water. As a consequence, we adopt, as a pH standard, a 0.01 m solution of HCl, as previously proposed [1]. Using the potential of a pH-sensitive electrode in the standard solution vs. a EPBRE, as a basis, we can then establish relationships between the pH and cell potential and hence develop a practical pH scale for supercritical systems. The results of these calculations and a comparison with experimental data are presented below.

Contribution of the Activity of Water

In order to interpret the results of EMF measurements at supercritical temperatures, we need to estimate the activity of water, which appears in the equation for the potential of the YSZ membrane electrode [5]:

$$E = E_{YSZ}^o - \frac{2.303RT}{F} pH - \frac{2.303RT}{2F} \log \frac{a_{H_2O}}{a_{H_2O}^o} \quad (6-1)$$

For supercritical water systems, which are essentially dense gases, we can use the concept of fugacity instead of activity. Fugacity is essentially pseudo pressure or corrected pressure, which permits the use of ideal gas equations for real gases. We can use the following relationship between fugacity (f) and activity of water:

$$\frac{a_{H_2O}}{a_{H_2O}^o} = \frac{f}{f^o} \quad (6-2)$$

where superscript "o" stands for a reference or standard state. There exist several means for estimating the fugacity of a gas. We have used the technique based on determining the difference between the isothermal expansion work functions for ideal and real gases [6]. Indeed, the work of isothermal expansion of an ideal gas from pressure P_2 to P_1 can be obtained as follows: $A_{id}=RT\ln(P_2/P_1)$. For a real gas, the same work should be written using fugacities (f): $A_{re}=RT\ln(f_2/f_1)$. The difference between A_{id} and A_{re} is the excess expansion work:

$$\Delta A = RT \ln \frac{P_2}{P_1} - RT \ln \frac{f_2}{f_1} = RT \ln \frac{P_2 f_1}{P_1 f_2} \quad (6-3)$$

We must choose as P_1 a suitably low pressure, such that the real gas behaves practically as an ideal gas. In that case, $P_1=f_1$ and ΔA becomes:

$$\Delta A = RT \ln \frac{P_2}{f_2} \quad (6-4)$$

From the last equation one obtains the fugacity as

$$f_2 = P_2 \exp\left(-\frac{\Delta A}{RT}\right) \quad (6-5)$$

and the fugacity coefficient is then given by:

$$\mathbf{g}_2 = \frac{f_2}{P_2} = \exp\left(-\frac{\Delta A}{RT}\right) \quad (6-6)$$

The value of ΔA is easily estimated as

$$\Delta A = A_{id} - A_{re} = \int_{P_2}^{P_1} V_{id} dP - \int_{P_2}^{P_1} V_{re} dP = \int_{P_2}^{P_1} (V_{id} - V_{re}) dP \quad (6-7)$$

Taking into account that for one mole of ideal gas $PV=RT$, we obtain:

$$\Delta A = \int_{P_2}^{P_1} \left(\frac{RT}{P} - V_{re}\right) dP \quad (6-8)$$

The values of ΔA were estimated for water at supercritical temperatures and at several P_2 values over the range 1-1000 bars from Equation (6-8) using specific volumes obtained from the ASME Steam Tables [7]. We chose water vapor at 1 bar and the corresponding temperature as the standard state.

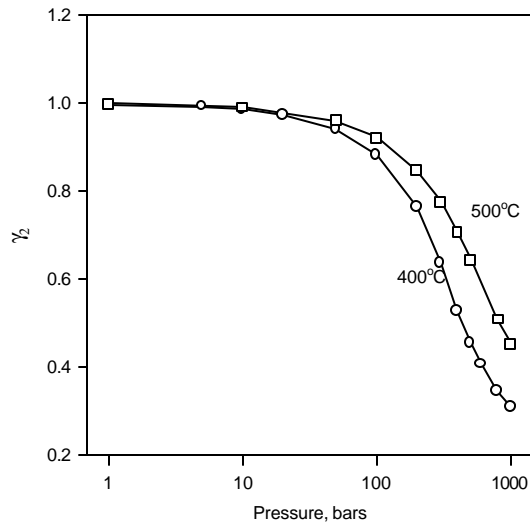


Figure 6-6. Calculated fugacity coefficient for water at 400 °C and 500 °C as a function of pressure.

Calculated values for γ_2 are presented in the Figure 6-6 for temperatures of 400 and 500°C. It is clear that the fugacity coefficient drops precipitously at pressures higher than 100 bars, especially so at low supercritical temperatures. An increase in temperature, as one would expect, makes the fluid more "ideal", so that at higher temperatures the fugacity coefficient decreases more slowly with pressure than at lower temperatures.

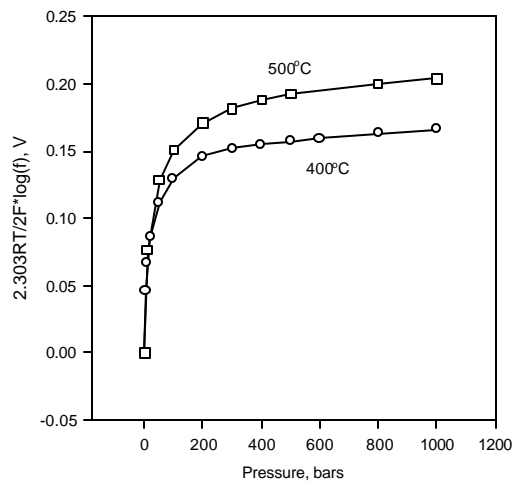


Figure 6-7. Calculated contribution of the fugacity of water to the potential of the cell YSZ/EPBRE at 400 °C and 500 °C as a function of pressure.

We emphasize here that the activities (fugacities) of water calculated above are related to pure water only. In order to obtain activities of water in solutions we need to employ PVT data for corresponding systems. However, for relatively dilute solutions, we can practically neglect the effect of the solute upon the properties of the solvent and use fugacity data calculated from properties of pure water.

We can now estimate the effect of fugacity on cell potential as

$$\Delta E = \frac{2.303 RT}{2F} \log f_{H_2O} \quad (6-9)$$

Values of ΔE are plotted vs. pressure in Figure 6-7 for temperatures of 400 and 500°C. We note that the effects of pressure are significant. Thus, for a change in pressure from 500 to 1000 bar at 500°C, the effect of the change in fugacity on cell potential would be $0.192 - 204 = -0.012$ V.

References

1. L. B. Kriksunov and D. D. Macdonald, "Understanding chemical conditions in supercritical water oxidation systems". Proceedings of the ASME Heat Transfer Division, 1995, Vol. 2), 271-279; 317(1995) (Am. Soc. Mech. Eng.).
2. L. B. Kriksunov and D. D. Macdonald, J. Electrochem. Soc. **141**, 3002 (1994).
3. L. B. Kriksunov and D. D. Macdonald, Sensors and Actuators B (Chemical), **22**, 201 (1995).
4. L. B. Kriksunov and D. D. Macdonald, Proc. 12th International Conference on the Properties of Water and Steam, Orlando FL, Sept. 1994, Begell House (1995).
5. D.D. Macdonald, S. Hettiarachchi, H. Song, K. Makela, R. Emerson, M. Haim, J. Solut. Chem. **21**, 849 (1992).
6. N.A. Izmailov, Electrochemistry of Solutions (in Russian), Khimia, Moscow (1976).
7. ASME Steam Tables, Sixth edition, ASME, N.Y. (1993).

7. Relevance, Impact, and Technology Transfer

The research reported in this document has made a significant contribution to the development of Super Critical Water Oxidation (SCWO) technology by devising methods for monitoring the chemical, electrochemical, and corrosion properties of the reaction environment. It is now well recognized that the principal hurdle that needs to be overcome in the development of SCWO technology is to identify materials that can withstand the extraordinarily aggressive reaction conditions that exist in the reactor or to modify the conditions such that existing materials may serve satisfactorily. The first option requires a method for quantitatively monitoring corrosion rate under the actual process conditions. The second option requires sensors that can be used to monitor the chemical and electrochemical conditions within the reaction zone, so that the conditions may be modified to minimize the accumulation of corrosion damage and yet maintain very high destruction efficiencies. Both requirements have been successfully addressed in this program with the first reported measurement of pH at realistic process temperatures ($T > 500$ °C) and the first demonstration that three electrode electrochemical noise measurements may be used to quantitatively monitor corrosion rate at super critical temperatures. Additionally, we have successfully developed high precision electrochemical techniques for measuring pH in high subcritical aqueous systems. These techniques yield "research grade" pH measurements and hence represent a quantum leap in the study of hydrolytic phenomena under high subcritical/super critical conditions. Indeed, we have demonstrated the efficacy of the methods by, for the first time, measuring potentiometrically the dissociation constant of HCl in high sub critical solutions (temperature up to 360 °C). Finally, we have applied the knowledge developed in this project to assist the US Army in selecting materials for use in the Newport, IN SCWO reactor that is now being developed for the destruction of VX hydrolysate. This important "technology transfer" to another government agency has contributed significantly to the attainment of their mission.

Items of specific impact and relevance are discussed in more detail below:

- **In-Situ Potentiometric Measurement of pH**

Advanced electrodes and sensors for in-situ potentiometric monitoring of pH in high subcritical and supercritical aqueous solutions have been developed. pH measurements of plant monitoring quality have been made at temperatures as high as 528 °C in both dilute acid (HCl) and alkaline (NaOH) environments. Additionally, we have demonstrated that the pH probes developed in this work can be used to monitor the destruction of a resilient organic waste (in this case carbon tetrachloride) under realistic process conditions. This is an important development, because it demonstrates, for the first time, that "pH" is a relevant chemistry control parameter in SCWO systems.

Additionally, an experimental thermocell was fabricated to test the flow-through reference electrode, the flow-through hydrogen electrode, and the flow-through YSZ pH sensor. An approach has been developed for the experimental evaluation of the association constants for 1-1 aqueous electrolytes using a flow-through electrochemical thermocell. The thermocell consists of a flow-through Pt(H₂) electrode and a flow-through external reference electrode. The viability of this method has been verified using previously obtained emf data for aqueous HCl solutions at temperatures from 300 to 360°C and for pressures of 27.5 and 33.8 MPa. The

derived values of the association constant of HCl(aq) are found to be in good agreement with literature data. pH values for 0.01 and 0.001 mol kg⁻¹ aqueous HCl solution are determined at temperatures and pressures of interest.

- **In-Situ Measurement of Corrosion Rate via ENA**

An electrochemical noise sensor have been developed for the *in-situ* measurement of corrosion rate in subcritical and supercritical conditions, and the sensor has been evaluated in a contamination-free, flow-through hydrothermal electrochemical cell. The following conclusions were drawn from the present results:

1. By measuring coupling current for a pair of identical metal electrodes, and by simultaneously measuring the potential of one of the electrodes against a reference electrode, the corrosion rate can be evaluated quantitatively, as has been demonstrated by many workers at lower temperatures.
2. The corrosion rate of Type 304 SS is a function of temperature and flow rate and the corrosion rate of Type 304 SS passes a maximum at 350°C, as determined by the results from both ENA and mass loss experiments. The existence of the maximum is in agreement with earlier corrosion activity (coupling current noise) measurements on both carbon steel and stainless steel in high subcritical and supercritical systems and with the predictions of a previously developed phenomenological model.
3. The proportionality between the inverse noise resistance and corrosion rate evaluated from mass loss tests exists in a wide range of conditions, i.e. temperatures from 150 to 390°C and for flow rate from 0.375 to 1.00 ml/min.
4. The Stern-Geary equation is a good approximation for the relationship between polarization resistance and corrosion current density for temperatures greater than 150°C.

- **Effect of Pressure on Corrosion Rate**

A model has been developed for estimating the effect of pressure on reaction rates, including corrosion rates, in high subcritical and supercritical aqueous systems. The model takes into account the effect of pressure on the activation process, on the volumetric concentration of the reactants, and on the dissociation of HCl. The predictions of the model have been tested against experimental data for the corrosion of Type 1013 carbon steel in oxygenated (0.006 ppm O₂) supercritical water (T = 481 °C) over the pressure range from 2500 psi to 3500 psi. Satisfactory agreement is obtained between theory and experiment. The model is then used to explore the effects of pressure excursions on materials selection experiments, with the following findings:

1. Positive pressure excursions are predicted to increase the corrosion rate due to positive effects on activation, volumetric concentration, and HCl dissociation. A maximum increase in the corrosion rate of about 60 % is predicted for the highest temperature considered (T = 371.1 °C) upon increasing the pressure by 35.72 b (525 psi).
2. Negative pressure excursions are predicted to decrease the corrosion rate due to negative effects on activation, volumetric concentration, and HCl dissociation. A decrease in the corrosion rate of about 14 % is predicted for the lowest temperature considered (T = 343.3 °C) upon decreasing the pressure by 61.24 b (900 psi). However, very large reductions in corrosion rate are predicted for the two highest temperatures (365.5 °C and 371.1 °C) upon decreasing the pressure in the system by 900 psi. This large decrease, which may be orders in magnitude, is due to the sharp decrease in the dielectric constant of the medium and hence is due to strong decreases in the dissociation constants for water and hydrochloric acid as the temperature approaches the critical value.

These calculations further suggest that considerable relief from corrosion may be obtained by operating the VX hydrolysate reactor at reduced pressures. However, this would be at the expense of through put.

- **Standardization of the pH Scale**

Following previous work, a pH standard for supercritical water has been developed, based upon the calculated values of the pH in a standard, 0.01 m HCl solution as a function of temperature. The importance of the activity of water in the measurement of pH at high temperatures is demonstrated.

8. Project Productivity

The principal goals of the study, the development of effective methods for monitoring chemical, electrochemical, and corrosion parameters in high sub critical and super critical aqueous systems, were achieved, as indicated above. The only task that could not be completed was the preliminary testing of the sensors in an actual SCWO reactor. This was due to the difficulty in scheduling time in the reactor at INEEL and due to the fact that the present sensors were judged to be too fragile for insertion into the pilot plant reactor. An assessment of the current state-of-the-art showed that considerable work remains to be done to ruggedize the sensors to the extent necessary for their use in a plant environment. A follow-on proposal to develop rugged sensors has been submitted to EMSP.

9. Personnel Supported

Digby D. Macdonald (PI), Professor, Dept. of Materials Science and Engineering, Pennsylvania State University.

Serguei N. Lvov (Co PI), Assoc. Professor, Dept. of Energy and Geo-Environmental Engineering, Pennsylvania State University.

X. Y. Zhou, Research Assoc., The Energy Institute, Pennsylvania State University.

X. Wei, Post Doctoral Scholar, The Energy Institute, Pennsylvania State University.

Serguei M. Ulyanov, Graduate Student, The Energy Institute, Pennsylvania State University.

10. Degrees Granted

Mr. Ulyanov will graduate with an MS degree (“pH Measurements and Potential-pH Diagram Calculations in High Temperature Subcritical and Supercritical Aqueous Solutions”) in May, 2001.

11. Publications and Presentations

Papers in press or in print:

1. S. N. Lvov and D. D. Macdonald, “Potentiometric Studies of Supercritical Water Chemistry”. In: *High Temperature Materials Chemistry* (ed. K.E. Spear), ECS, pp. 746-754 (1997).
2. S. N. Lvov and D. D. Macdonald, “Thermodynamic Computer Simulation of Hydrothermal Synthesis of Oxides in Supercritical Aqueous Environments”. In: *High Temperature Materials Chemistry* (ed. K.E. Spear), ECS, pp. 472-479 (1997).
3. G. R. Engelhardt, S. N. Lvov, and Macdonald, “Importance of Thermal Diffusion Transport in Electrochemical Cells in High Temperature Aqueous Solutions”, *J. Electroanal. Chem.*, pp. 193-201 (1997).
4. A. V. Bandura, S. N. Lvov, and D. D. Macdonald, “Thermodynamics of Ion Solvation in Dipolar Solvent Using Monte Carlo Mean Reaction Field Approximation”, *J. Chem. Soc. Faraday Trans.*, **94**, 1063-1072 (1998).
5. S. N. Lvov, X. Y. Zhou, and D. D. Macdonald, “Flow-Through Electrochemical Cell for Accurate pH measurements at Temperatures up to 400°C”. *J. Electroanal. Chem.*, **463**, 146-156 (1999).
6. S. N. Lvov, X. Y. Zhou, S. M. Ulyanov, and D. D. Macdonald, “Potentiometric Measurements of Association Constant and pH in High Temperature HCl (aq) solutions”, In: *Steam, Water, and Hydrothermal Systems: Physics and Chemistry. Meeting the Needs of Industry*, Eds. P. P.R. Tremaine, P.G. Hill, D.E. Irish, and P.V. Palakrishnan, NRC Press Ottawa, 2000, p. 480.
7. S. N. Lvov and X. Y. Zhou, “pH Measurements in Supercritical Hydrothermal Systems”, *Miner. Mag.*, **62A**, 929-930 (1998).
8. S. N. Lvov, M. M. Ulyanova, G. R. Engelhardt, and D. D. Macdonald, “Importance of Thermal Diffusion in High Subcritical and Supercritical Aqueous Solutions”, *Int. J. Thermophysics*, **19**, 1567-1575 (1998).
9. X.Y. Zhou, S.N. Lvov, X.J. Wei, and L. G. Benning, and D.D. Macdonald, “Quantitative Evaluation of General Corrosion of Type 304 Stainless Steel in Subcritical and Supercritical Aqueous Solutions Via Electrochemical Noise Analysis”, *Corrosion Science*, in press (2001).

10. S.N. Lvov, H. Gao, and D.D. Macdonald, "Advanced Flow Through External Pressure Balanced Reference Electrode for Potentiometric and pH Studies in High Temperature Aqueous Solutions", *J. Electroanal. Chem.*, **443**, 186-194 (1998).
11. S.N. Lvov, H. Gao, D. Kouznetsov, I. Balachov and D. D. Macdonald, "Potentiometric pH Measurements in High Subcritical and Supercritical Aqueous Solutions", *Fluid Phase Equilibria*, **150/151**, 515-523 (1998).
12. S.N. Lvov, X.Y. Zhou, and D.D. Macdonald, *J. Electroanal. Chem.*, "Flow-Through Electrochemical Cell for Accurate pH Measurements at Temperatures up to 400 °C", **463**, 146-156 (1999).
13. S.N. Lvov, X.Y. Zhou, S. M. Ulyanov, and A.V. Bandura, "Reference System for Assessing Viability and Accuracy of pH Sensors in High Temperature Subcritical and Supercritical Aqueous Solutions", *Chemical Geology*, **167**, 105-115 (2000).
14. D. D. Macdonald, "An Overview of the Chemical and Electrochemical Conditions that Exist in SCWO Systems," *Corrosion 2001*, Houston, TX, March 11-16, 2001 (printed paper).
15. D. D. Macdonald and L. B. Kriksunov, "Probing the Chemical and Electrochemical Properties of SCWO Systems", *Electrochim. Acta*, 2001 (in press).
16. X. Y. Zhou, A. V. Bandura, S. M. Ulyanov, and S. N. Lvov, "Calculation of Diffusion Potentials in Aqueous Solutions Containing HCl, NaOH, and NaCl at Temperatures from 25 to 400°C". In: *Steam, Water, and Hydrothermal Systems: Physics and Chemistry. Meeting the Needs of Industry*, Eds. P.R. Tremaine, P.G. Hill, D.E. Irish, and P.V. Palakrishnan, NRC Press, Ottawa, 2000 (in press).
17. S. N. Lvov, X. Y. Zhou, and S. M. Ulyanov, "Developing pH Reference Systems for High Temperature Subcritical and Supercritical Aqueous Solutions", *Chemical Geology*, 1999 (submitted).

Papers in preparation:

1. Macdonald, D. D., "Effect of Pressure on the Rates of Corrosion Processes in Super Critical Aqueous Systems", *Corrosion Science*, 2001 (in preparation).

Conference presentations and invited seminars:

1. D. D. Macdonald, "Chemistry Sensors for the Universal Solvents-Supercritical Aqueous Solutions." Proceedings of the 4th International Symposium on Supercritical Fluids, p.861-864, May 11-14, 1997, Sendai, Japan.
2. S. N. Lvov, X. Y. Zhou, and D. D. Macdonald, "Potentiometric pH Measurements in Supercritical Aqueous Solutions", The 193rd Meeting of The Electrochemical Society, Inc., Abstracts No. 1016, May 3-8, 1998.
3. D. D. Macdonald, S. N. Lvov, and L. B. Kriksunov, "The chemical and Electrochemical Properties of Supercritical Aqueous Solutions". The 193rd Meeting of The Electrochemical Society, Inc., Abstract No. 1012, May 3-8, San Diego, 1998.
4. S. N. Lvov, X. Y. Zhou, X. J. Wei, S. M. Ulyanov, and D. D. Macdonald, "Electrochemical Corrosion Studies in High Temperature Subcritical and Supercritical Aqueous Environments". The 218th American Chemical Society Meeting, Abstract No. 129, August 22-26, New Orleans, 1999.
5. D. D. Macdonald, "The Chemistry and Electrochemistry of High Subcritical and Supercritical Aqueous Systems", Distinguished Lecturer Series, University of Toronto, Toronto, Canada, November 10, 1999.

Invention Disclosures

1. Zhou X.Y., Lvov S.N., Ulyanov S.M. "Safe Yttria-Stabilized Zirconia (YSZ) pH Sensing Electrode for High Temperature Aqueous Systems" Invention Disclosure No. 98-1989, November 11, 1998.